

Deriving a sea surface CO₂ climatology

L. M. Goddijn-Murphy
et al.

Deriving a sea surface climatology of CO₂ fugacity in support of air–sea gas flux studies

L. M. Goddijn-Murphy¹, D. K. Woolf², P. E. Land³, J. D. Shutler³, and C. Donlon⁴

¹ERI, University of the Highlands and Islands, Ormlie Road, Thurso, UK

²ICIT, Heriot-Watt University, Stromness, UK

³Plymouth Marine Laboratory, Prospect Place, Plymouth, UK

⁴European Space Agency/ESTEC, Noordwijk, the Netherlands

Received: 27 June 2014 – Accepted: 8 July 2014 – Published: 28 July 2014

Correspondence to: L. M. Goddijn-Murphy (lonneke.goddijn-murphy@uhi.ac.uk)

Published by Copernicus Publications on behalf of the European Geosciences Union.

Title Page

Abstract

Introduction

Conclusions

References

Tables

Figures

◀

▶

◀

▶

Back

Close

Full Screen / Esc

Printer-friendly Version

Interactive Discussion



Abstract

5 Climatologies, or long-term averages, of essential climate variables are useful for evaluating models and providing a baseline for studying anomalies. The Surface Ocean Carbon Dioxide (CO₂) Atlas (SOCAT) has made millions of global underway sea surface measurements of CO₂ publicly available, all in a uniform format and presented as fugacity, f_{CO_2} . f_{CO_2} is highly sensitive to temperature and the measurements are only valid for the instantaneous sea surface temperature (SST) that is measured concurrent with the in-water CO₂ measurement. To create a climatology of f_{CO_2} data suitable for calculating air–sea CO₂ fluxes it is therefore desirable to calculate f_{CO_2} valid for climate quality SST. This paper presents a method for creating such a climatology. We recomputed SOCAT's f_{CO_2} values for their respective measurement month and year using climate quality SST data from satellite Earth observation and then extrapolated the resulting f_{CO_2} values to reference year 2010. The data were then spatially interpolated onto a 1° × 1° grid of the global oceans to produce 12 monthly f_{CO_2} distributions for 2010. The partial pressure of CO₂ (p_{CO_2}) is also provided for those who prefer to use p_{CO_2} . The CO₂ concentration difference between ocean and atmosphere is the thermodynamic driving force of the air–sea CO₂ flux, and hence the presented f_{CO_2} distributions can be used in air–sea gas flux calculations together with climatologies of other climate variables.

20 1 Background

1.1 Introduction

25 Observations demonstrate that dissolved CO₂ concentrations in the surface ocean have been increasing nearly everywhere, roughly following the atmospheric CO₂ increase but with large regional and temporal variability (Takahashi et al., 2009; McKinley et al., 2011). In general, tropical waters release CO₂ to the atmosphere, whereas

OSD

11, 1895–1948, 2014

Deriving a sea surface CO₂ climatology

L. M. Goddijn-Murphy et al.

Title Page

Abstract

Introduction

Conclusions

References

Tables

Figures

◀

▶

◀

▶

Back

Close

Full Screen / Esc

Printer-friendly Version

Interactive Discussion



Deriving a sea surface CO₂ climatology

L. M. Goddijn-Murphy et al.

Title Page

Abstract

Introduction

Conclusions

References

Tables

Figures

◀

▶

◀

▶

Back

Close

Full Screen / Esc

Printer-friendly Version

Interactive Discussion



state that SST_{depth} should always be quoted at a specific depth in the water column; e.g., SST_{5m} refers to the SST at a depth of 5 m. However, SST_{depth} data can be measured using a variety of different temperature sensors mounted on buoys, profilers and ships at any depth beneath the water skin and the depth of the measurement is often not recorded. Different measurement systems that are used to measure SST (e.g. hull mounted thermistors, inboard thermosalinograph systems) have evolved over time using different techniques that are prone to different error characteristics (e.g. for a good review see Kennedy, 2013; Kennedy et al., 2011a, b), such as warming of water as it passes through the ships' internal pipes before reaching an inboard thermosalinograph (e.g. Kent et al., 1993; Emery et al., 2001; Reynolds et al., 2010; Kennedy, 2013), poor calibration or biases due to the location and warming of hull mounted temperature sensors (e.g. Emery et al., 1997, 2001), inadequate knowledge of temperature sensor depth (e.g. Emery et al., 1997; Donlon et al., 2007), poor knowledge of temperature sensor calibration performance and local thermal stratification during a diurnal cycle (e.g., Kawai and Wada, 2007). This means that if not carefully controlled, SST biases of > 1 K may easily be introduced into an in situ SST dataset.

All of these issues mean that directly using SST and f_{CO_2} measurement pairs from a large dataset (i.e., that resulting from a large number of different instrument setups and methods) to a f_{CO_2} climatology for studying air–sea gas fluxes is likely to introduce a source of error. Therefore, we propose that correcting all of the f_{CO_2} data back to a consistent surface SST dataset is clearly advantageous and this is where satellite data can provide help.

1.3 The use of satellite sea surface temperature data

Satellite Earth observation thermal infrared radiometers used to sense sea skin temperature variations have been in orbit around the Earth since the 1990s. The resultant data are calibrated to skin temperature (rather than SST at depth) and have been shown to have a higher accuracy and precision for studying SST than in situ methods (e.g., O'Carroll et al., 2008) and such data are now available as a climate data record

Deriving a sea surface CO₂ climatology

L. M. Goddijn-Murphy
et al.

Title Page

Abstract

Introduction

Conclusions

References

Tables

Figures

◀

▶

◀

▶

Back

Close

Full Screen / Esc

Printer-friendly Version

Interactive Discussion



approximation of the water temperature in the meters below the surface, SST_{depth} (Donlon et al., 1999; 2002). According to Kettle et al. (2009) the difference between f_{CO_2} for the temperature at the base of the mass boundary layer, and f_{CO_2} for SST_{depth} is negligible so we calculated f_{CO_2} using subskin SST to estimate f_{CO_2} at the base of the mass boundary layer. The ARC dataset provides SST_{skin} from infrared imagery gridded to a 0.1° latitude–longitude resolution (Merchant et al., 2012). For each year from August 1991 to December 2010 Oceanflux GHG derived 12 monthly mean SST_{skin} distributions, averaged over a 1° × 1° grid without differentiating between day- and night-time measurements (<http://www.oceanflux-ghg.org/Products/OceanFlux-data/Monthly-composite-datasets>). These SST_{skin} grid points were linearly interpolated to the SOCAT measurement locations (SST_{skin,i}). We defined T_{ym} as the single year, monthly 1° × 1° grid box mean of $T_{\text{ym},i} = \text{SST}_{\text{skin},i} + 0.14$. The f_{CO_2} values were re-computed from in situ SST to $T_{\text{ym},i}$ for our climatology (Sect. 3.2).

With SST the corresponding grid box mean of SOCAT's in situ SST (generally obtained at 5 m nominal depth) and using all data from the years 1991 to 2007, a histogram of $dT = T_{\text{ym}} - \text{SST}$ was produced (Fig. 1). It shows dT was distributed around a mean of -0.09 with a standard deviation of 0.55. This difference implied that the gridded in situ SST systematically overestimated T_{ym} . The corresponding histogram of our correction $f_{\text{CO}_2}(T_{\text{ym}}) - f_{\text{CO}_2}(\text{SST})$ (not shown) revealed a similar distribution around $-1.12 \mu\text{atm}$. The temperature differences were found to be positive as well as negative (Fig. 1). Positive dT can be a consequence of diurnal warming when the top layer heats up by solar radiation during the day. This heat is lost again during the night. Cooling of the top layer (negative dT) is a less described phenomenon but can be expected in colder environments. We found more negative dT during the winter months and at high latitudes. The temperature profile in the sea depends on wind speed as wind mixes the water column, i.e. for strong winds SST is expected to be more constant in the vertical. We illustrate the wind speed dependence of dT for the North Atlantic because this region has the highest SOCAT data density. For each dT we retrieved the monthly 1° × 1° grid box mean of 10 m wind speed, U_{10} (m s^{-1}), from Oceanflux

GHG's composite of GlobWave merged altimeter data (<http://www.oceanflux-ghg.org/Products/OceanFlux-data/Monthly-composite-datasets>). A scatter plot of dT as a function of U_{10} , averaged over in 1 m s^{-1} U_{10} bins, (Fig. 2) showed that dT decreased with increasing U_{10} becoming negative for wind speeds over about 10 m s^{-1} . Similar trends were seen in the other regions, but with dT turning negative for different wind speeds: North Pacific 9 m s^{-1} ; Coastal 8 m s^{-1} ; Tropical Atlantic and Southern Ocean 6 m s^{-1} ; Tropical Pacific, Indian Ocean and Arctic 4 m s^{-1} (SST data from Bakker et al., 2013). The Tropical Atlantic was different in that dT became less negative for wind speed over $\sim 8 \text{ m s}^{-1}$, turning positive over $\sim 10 \text{ m s}^{-1}$. If only North Atlantic data from the winter months December, January and February were included, nearly all dT values would be negative.

1.5 The OceanFlux climatology of f_{CO_2} and SST

We have converted the SOCAT's instantaneous f_{CO_2} (and SST) data to a monthly mean f_{CO_2} using a climate data record of SST. This approach has only recently become possible due to the availability of the consistently calibrated sea surface temperature climate record (Merchant, 2008, 2012). In order to eliminate biases due to the sampling year (i.e., surface ocean f_{CO_2} has been increasing over the years) f_{CO_2} values from all years were extrapolated to reference year 2010 using a simple linear relationship.

2 The SOCAT database

2.1 Introduction

The SOCAT database contains millions of surface ocean CO_2 measurements in all ocean areas spanning four decades. All data are put in a uniform format while clearly defined criteria are applied in their quality control. SOCAT has been made possible through the cooperation (data collection and quality control) of the international marine

Deriving a sea surface CO_2 climatology

L. M. Goddijn-Murphy et al.

Title Page

Abstract

Introduction

Conclusions

References

Tables

Figures



Back

Close

Full Screen / Esc

Printer-friendly Version

Interactive Discussion



carbon science community. The history and organisation of SOCAT is described in Pfeil et al. (2013). SOCAT version 1.5 includes 6.3 million measurements from 1968 to 2007 and was made publicly available in September 2011 at <http://www.socat.info/SOCATv1/>. SOCAT data is available as three types of data products: individual cruise files, gridded products and merged synthesis data files. For our study we used the latter and we downloaded the individual regional synthesis files from <http://cdiac.ornl.gov/ftp/oceans/SOCATv1.5/>. The content of these files (parameter names, units and descriptions) are described in Table 5 in Pfeil et al. (2013). The data can be displayed in the online Cruise Data Viewer (Fig. 3) and downloaded in text format.

2.2 The SOCAT computation of SOCAT fugacity in seawater

The collected CO_2 concentrations are expressed as mole fraction, x_{CO_2} , partial pressure, p_{CO_2} , or fugacity, f_{CO_2} , of CO_2 . SOCAT's re-computation is to achieve a uniform representation of the CO_2 measurements and all measurements are converted to fugacity in seawater $f_{\text{CO}_2,\text{is}}$ (fCO2_rec) for in situ sea surface, SST (temp). The parameters in brackets refer to their SOCAT version 1.5 names (Table 5 in Pfeil et al., 2013). SST is the intake temperature which signifies $\text{SST}_{\text{depth}}$. The shipboard measurements were taken at equilibrator temperature T_{eq} (Temperature_equi) and equilibrator pressure, P_{eq} (Pressure_equi). SOCAT calculates $f_{\text{CO}_2,\text{is}}$ from $p_{\text{CO}_2,\text{is}}$, partial pressure in seawater corrected for the difference between SST and the temperature at the equilibrator, using Eqs. (1) and (2)

$$p_{\text{CO}_2,\text{is}} = p_{\text{CO}_2}(T_{\text{eq}}) \exp(0.0423(\text{SST} - T_{\text{eq}})) \quad (1)$$

$$f_{\text{CO}_2,\text{is}} = p_{\text{CO}_2,\text{is}} \exp \left(\frac{\left[B(\text{CO}_2, \text{SST}) + 2(1 - x_{\text{CO}_2,\text{wet}}(T_{\text{eq}}))^2 \delta(\text{CO}_2, \text{SST}) \right] P_{\text{eq}}}{R \cdot \text{SST}} \right) \quad (2)$$

with $B(\text{CO}_2, \text{SST})$ and $\delta(\text{CO}_2, \text{SST})$ calculated from Weiss (1974):

$$B(\text{CO}_2, T) = -1636.75 + 12.0408T - 3.27957 \times 10^{-2}T^2 + 3.16528 \times 10^{-5}T^3 \quad (3)$$

$$\delta(\text{CO}_2, T) = 57.7 - 0.118T \quad (4)$$

(Pfeil and Olsen, 2009). In Eqs. (1)–(4) f_{CO_2} and p_{CO_2} are in μatm , P_{eq} in hPa, temperatures are in kelvins and $x_{\text{CO}_2, \text{wet}}(T_{\text{eq}})$ is the wet mole fraction as parts per million (ppm) of CO_2 at equilibrator. The gas constant $R = 82.0578 \text{ cm}^3 \text{ atm (mol K)}^{-1}$. How $p_{\text{CO}_2}(T_{\text{eq}})$ is measured, the temperature correction (Eq. 1) and the necessarily different starting points of the computation are discussed in respective Sects. 2.3–2.5. Our conversion, from the given $f_{\text{CO}_2, \text{is}}$ calculated for in situ measurements to climatological $f_{\text{CO}_2, \text{cl}}$ in 2010 is explained in Sect. 3.

2.3 Measurements of $p_{\text{CO}_2}(T_{\text{eq}})$

The measurement method of p_{CO_2} in seawater described by Takahashi et al. (2009) is summarized in the following. On board the ship carrier gas is equilibrated with streaming seawater in the headspace of an equilibrator and the concentration of CO_2 in the equilibrated carrier gas is measured. When a dry carrier gas is analysed, seawater $p_{\text{CO}_2}(T_{\text{eq}})$ in the equilibrator chamber is computed using

$$p_{\text{CO}_2}(T_{\text{eq}}) = x_{\text{CO}_2, \text{dry}}(P_{\text{eq}} - P_{\text{w}}) \quad (5)$$

where P_{eq} is the pressure at the equilibrator, P_{w} water vapour pressure at T_{eq} and salinity (S), and $x_{\text{CO}_2, \text{dry}}$ the mole fraction of CO_2 in dry air. P_{w} is calculated with

$$P_{\text{w}} = \exp(24.4543 - 67.4509(100/T_{\text{eq}}) - 4.8489(\ln(T_{\text{eq}}/100) - 0.000544S) \quad (6)$$

with T_{eq} in Kelvin and S the sample salinity (Pfeil and Olsen, 2009). When mixing ratios in a wet carrier gas (100 % humidity) are determined, P_{w} is set to zero

$$p_{\text{CO}_2}(T_{\text{eq}}) = x_{\text{CO}_2, \text{wet}}P_{\text{eq}} \quad (7)$$

Deriving a sea surface CO_2 climatology

L. M. Goddijn-Murphy et al.

Title Page

Abstract

Introduction

Conclusions

References

Tables

Figures

◀

▶

◀

▶

Back

Close

Full Screen / Esc

Printer-friendly Version

Interactive Discussion



2.4 Temperature handling

There are different methods to correct for the difference in partial pressure at intake and equilibrator temperature. SOCAT uses the simple Eq. (1) (Pfeil and Olsen, 2009); they refer to more complicated methods but disregard these because they require knowledge of the total dissolved inorganic carbon, T_{CO_2} , and alkalinity, T_{Alk} , and are not determined for isochemical conditions. Takahashi et al. (2009) use

$$p_{\text{CO}_2,\text{is}} = p_{\text{CO}_2}(T_{\text{eq}}) \exp \left(0.0433(\text{SST} - T_{\text{eq}}) - 4.35 \times 10^{-5} (\text{SST}^2 - T_{\text{eq}}^2) \right) \quad (8)$$

with SST and T_{eq} in °C. Equations (1) and (8) correct for the effect of slight warming before measurement at the equilibrator on an isochemical transformation (T_{CO_2} and T_{Alk} are unchanged but pH and aqueous CO_2 concentration may vary). Equation (8) is an integrated form of

$$\delta \ln(p_{\text{CO}_2}) / \delta T = 0.0433 - 8.7 \times 10^{-5} T$$

while in Eq. (1) a mean coefficient of $0.0423 \text{ } ^\circ\text{C}^{-1}$ is used. Equation (8) was therefore expected to give more accurate $p_{\text{CO}_2,\text{is}}$ estimates.

2.5 Starting points of the SOCAT computation

Different measured parameters are available in different records to use as starting point for the SOCAT re-computation of $f_{\text{CO}_2,\text{is}}$ (Table 4 in Pfeil et al., 2013). Therefore SOCAT applies the following strict guidelines:

1. recalculate f_{CO_2} whenever possible;
2. order of preference of the starting point is: x_{CO_2} , p_{CO_2} , f_{CO_2} ;
3. minimize the use of external data.

Deriving a sea surface CO_2 climatology

L. M. Goddijn-Murphy
et al.

Title Page

Abstract

Introduction

Conclusions

References

Tables

Figures

◀

▶

◀

▶

Back

Close

Full Screen / Esc

Printer-friendly Version

Interactive Discussion



Deriving a sea surface CO₂ climatology

L. M. Goddijn-Murphy
et al.

Title Page

Abstract

Introduction

Conclusions

References

Tables

Figures

◀

▶

◀

▶

Back

Close

Full Screen / Esc

Printer-friendly Version

Interactive Discussion



The majority of the cases (57.5%) is derived from $x_{\text{CO}_2, \text{dry}}(T_{\text{eq}})$. However, in many cases only $f_{\text{CO}_2, \text{is}}$ (8.4%) or $p_{\text{CO}_2, \text{is}}$ (13.8%) was provided so that it is not certain that Eq. (1) was used by the cruise scientists to convert $p_{\text{CO}_2}(T_{\text{eq}})$ to $p_{\text{CO}_2, \text{is}}$. Moreover, if only $f_{\text{CO}_2, \text{is}}$ was reported, but pressure and salinity were not, $f_{\text{CO}_2, \text{is}}$ is not recalculated and $f_{\text{CO}_2, \text{is}}$ is taken as provided. The regional synthesis files only contain re-computed $f_{\text{CO}_2, \text{is}}$ values and don't give direct information about starting points other than which one was used (`fCO2_source`). However, each record contains a field "doi", indicating the digital object identifier to a publically accessible online data file in the PANGAEA database (<http://www.pangaea.de/>) where the original measurements before re-computation can be found. The individual cruise data files also contain various x_{CO_2} , p_{CO_2} , and f_{CO_2} data (Table 5 in Pfeil et al., 2013). Because we wanted to use SOCAT's uniform database, and not re-create it, we estimated $f_{\text{CO}_2, \text{cl}}$ from the $f_{\text{CO}_2, \text{is}}$ values in the merged synthesis files as explained in Sect. 3. An estimation of the errors in re-computed $f_{\text{CO}_2, \text{cl}}$ due to varying starting points is given in Sects. 5.6 and 5.7.

3 Our re-computation for climatological fugacity in the year 2010

3.1 Inversion: conversion of $f_{\text{CO}_2, \text{is}}$ to $p_{\text{CO}_2}(T_{\text{eq}})$

We used Eqs. (2) and (8) (with $\text{SST} = T_{\text{ym}, i}$) to calculate $f_{\text{CO}_2, \text{ym}, i}$ but because mole fraction $x_{\text{CO}_2, \text{is}}$, and partial pressures $p_{\text{CO}_2, \text{is}}$ and $p_{\text{CO}_2}(T_{\text{eq}})$ are not given in the SOCAT regional synthesis files, the first step was to estimate the original measurement of $p_{\text{CO}_2}(T_{\text{eq}})$. First $p_{\text{CO}_2, \text{is}}$ was derived from $f_{\text{CO}_2, \text{is}}$ by inverting Eq. (2):

$$p_{\text{CO}_2, \text{is}} = f_{\text{CO}_2, \text{is}} \exp \left(- \frac{[B + 2(1 - x_{\text{CO}_2, \text{wet}}(T_{\text{eq}}))^2 \delta] P_{\text{eq}}}{R \cdot \text{SST}} \right) \quad (9)$$

with $B = B(\text{CO}_2, \text{SST})$ and $\delta = \delta(\text{CO}_2, \text{SST})$ from Eqs. (3) and (4) and SST the SOCAT measurement. Defining $x_{\text{CO}_2, \text{wet}}(T_{\text{eq}})$ as $p_{\text{CO}_2}(T_{\text{eq}})/P_{\text{eq}}$ (Eq. 7) and writing $p_{\text{CO}_2}(T_{\text{eq}})$ in 1907

terms of $p_{\text{CO}_2,\text{is}}$ (Eq. 1), Eq. (9) leads to

$$p_{\text{CO}_2,\text{is}} = f_{\text{CO}_2,\text{is}} \exp \left(- \frac{\left[B + 2 \left(1 - \frac{p_{\text{CO}_2,\text{is}} \exp(-0.0423(\text{SST} - T_{\text{eq}}))}{P_{\text{eq}}} \right)^2 \delta \right] P_{\text{eq}}}{R \cdot \text{SST}} \right). \quad (10)$$

Equation (10) was solved with an iterative calculation

$$[p_{\text{CO}_2,\text{is}}]_{n+1} = f_{\text{CO}_2,\text{is}} \exp(g([p_{\text{CO}_2,\text{is}}]_n, \text{SST}, T_{\text{eq}}, P_{\text{eq}})) \quad (11)$$

(with g a function describing the exponent). In the first iteration the initial guess of $[p_{\text{CO}_2,\text{is}}]_1$ was $f_{\text{CO}_2,\text{is}}$ and the result $[p_{\text{CO}_2,\text{is}}]_2$ was put back in the right hand side of Eq. (11). This step was repeated until $|[p_{\text{CO}_2,\text{is}}]_N - [p_{\text{CO}_2,\text{is}}]_{N-1}| < 2^{-52}$. Using Eq. (1) we could then estimate the original $p_{\text{CO}_2}(T_{\text{eq}})$,

$$p_{\text{CO}_2}(T_{\text{eq}}) = p_{\text{CO}_2,\text{is}} \exp(-0.0423(\text{SST} - T_{\text{eq}})) \quad (12)$$

3.2 Conversion of $p_{\text{CO}_2}(T_{\text{eq}})$ to $f_{\text{CO}_2,\text{cl}}$ in the year 2010

The next step was to convert partial pressure at equilibrator temperature to partial pressure at $T_{\text{ym},i}$ for each SOCAT measurement. Because ARC ATSR data were available from August 1991 we converted SOCAT data from then onwards. As a consequence 95249 (1.4 %) of valid f_{CO_2} observations were not used from the SOCAT v1.5 dataset (from 119 cruises spread all over the globe). We note that the ESA CCI project is now working on an extended SST climate data record from satellite extending back to 1981 which is expected in 2015. Following Takahashi et al. (2009) we used Eq. (8) to correct for the difference between climatological and equilibrator temperature

$$p_{\text{CO}_2,\text{ym},i} = p_{\text{CO}_2}(T_{\text{eq}}) \exp \left(0.0433(T_{\text{ym},i} - T_{\text{eq}}) - 4.35 \times 10^{-5} (T_{\text{ym},i}^2 - T_{\text{eq}}^2) \right) \quad (13)$$

Deriving a sea surface CO₂ climatology

L. M. Goddijn-Murphy et al.

Title Page

Abstract

Introduction

Conclusions

References

Tables

Figures

◀

▶

◀

▶

Back

Close

Full Screen / Esc

Printer-friendly Version

Interactive Discussion



used the same variogram as for $f_{\text{CO}_2,\text{cl}}$ because the difference with $f_{\text{CO}_2,\text{cl}}$ was negligible compared to the spatial variation.

We applied ordinary kriging on mask map locations because it is the default action when observations, variogram, and prediction locations are specified (Pebesma, 1999). We performed local ordinary block kriging on a $1^\circ \times 1^\circ$ mask map of the global oceans with $\text{min} = 4$, $\text{max} = 20$, and $\text{radius} = 60$. Thus, after selecting all data points at (euclidian) distances from the prediction location less or equal to 60, the 20 closest were chosen when more than 20 were found and a missing value was generated if less than 4 points were found. The data were smoothed by averaging over square shaped 5×5 sized blocks. Thus gstat produced the $f_{\text{CO}_2,\text{cl}}$ (and $\rho_{\text{CO}_2,\text{cl}}$) prediction and variance values located at the grid cell centres of the (non-missing valued) cells in the grid map mask. These results were compared with results from different kriging options min, max, radius and block size (Sect. 5.3).

Our approach was simpler than the spatial interpolation on a $4^\circ \times 5^\circ$ grid of Takahashi et al. (2009). For each day they increase pixel size to four neighbouring pixels over 3 days (past, present and future day). The values of the pixels that are still without observations after this procedure are computed by a continuity equation based on a 2-D diffusion–advection transport equation for surface waters. All daily pixel values are used to calculate monthly mean values. Takahashi et al. (2009) estimate that the global mean surface water $\rho_{\text{CO}_2,\text{cl}}$ obtained in their study may be biased by about $+1.3 \mu\text{atm}$ due to under sampling and the interpolation method. The spatial interpolation method we applied is expected to give unbiased results (Pebesma, 1999).

5 Results

5.1 Monthly global maps

The prediction distributions of $f_{\text{CO}_2,\text{cl}}$ produced by the ordinary block kriging are shown in Fig. 5 for all 12 months. The maps showing the standard deviations of the kriging

Deriving a sea surface CO₂ climatology

L. M. Goddijn-Murphy et al.

Title Page

Abstract

Introduction

Conclusions

References

Tables

Figures

◀

▶

◀

▶

Back

Close

Full Screen / Esc

Printer-friendly Version

Interactive Discussion



Deriving a sea surface CO₂ climatology

L. M. Goddijn-Murphy
et al.

Title Page

Abstract

Introduction

Conclusions

References

Tables

Figures

◀

▶

◀

▶

Back

Close

Full Screen / Esc

Printer-friendly Version

Interactive Discussion



for January (all months) are shown in Fig. 6 (Fig. A1). The 12 monthly global distribution data have been made available in 12 netCDF-3 files in the Supplement related to this article. These files contain $f_{\text{CO}_2,\text{cl}}$, $p_{\text{CO}_2,\text{cl}}$, their spatial interpolation errors, and ARC's SST_{skin} for the year 2010, all on a $1^\circ \times 1^\circ$ grid. The variable names are respectively fCO2_2010_krig_pred, pCO2_2010_krig_pred, fCO2_2010_krig_std, pCO2_2010_krig_std, and Tcl_2010 (T_{ym} as defined in Sect. 1.4 for the year 2010). Monthly gridded values of atmospheric CO₂ dry air mole fractions in 2010, made available by the NOAA ESRL Carbon Cycle Cooperative Global Air Sampling Network (Dlugokencky et al., 2014), are also given as variable vCO2_2010. These were not used in our conversion but can help calculate air-sea gas CO₂ fluxes (Takahashi, 2009). The important differences with the Takahashi climatology are summarized in Table 1.

A range of errors needs to be considered when interpreting the final monthly maps. It is difficult to be complete but we considered the following errors. The spatial interpolation errors were estimated by taking the square root of the variances of the kriging. The different kriging approaches themselves were evaluated by calculating the mean and standard deviations of the varying $f_{\text{CO}_2,\text{cl}}$ kriging results using the options shown in Table 2. The cruises were bootstrapped to investigate if certain cruises dominated the mapped results. Other errors that were analysed were the “temporal extrapolation error”, the “inversion error” related to the different starting points, the consequences of the missing values, and the propagations of the uncertainties in the SOCAT measurements and $T_{\text{ym},i}$. These errors are discussed in the next sub sections and the final sub section gives a summary overview.

5.2 Spatial interpolation errors

The standard deviations (SD) of the applied kriging were calculated by taking the square root of the variance values produced by gstat (Pebesma, 1999). Kriging errors were obviously related to the available SOCAT data density in the measurement month (e.g., Fig. 3). The $f_{\text{CO}_2,\text{cl}}$ kriging SD mapped for all months are illustrated in Fig. A1. The monthly SD over all grid points was $20 \pm 5 \mu\text{atm}$ on average (mean over all monthly

means \pm Sd). The average monthly minimum and maximum SD values were 6.3 ± 2.6 and $50 \pm 8.7 \mu\text{atm}$. Problem areas emerged where no SOCAT data were available, for example in the western Southern Ocean and the Arctic. Spatial interpolation errors were lowest in the North Atlantic and North Pacific where SOCAT data was dense.

5 The month April showed the highest errors, this could be a consequence of the variogram range, c , being the smallest (implying that the covariance between the locations dropped quickly with distance). Our variogram model of combination of a nugget and a spherical model did not fit November data well as the semivariance was almost independent of distance; the low standard deviations in November (Fig. A1) were therefore probably not representative of the true error due to the kriging method. Standard deviations of the kriging are included in our presented data files; a bias is not supposed to be introduced by the kriging itself (Pebesma, 1999).

5.3 A comparison of the different kriging approaches

15 The ordinary block kriging of the $f_{\text{CO}_2, \text{cl}}$ data was repeated using a range of sensible kriging parameters (Table 2). The standard deviation of the mean over the different kriging results (Figs. 7 and A2) was less than $5 \mu\text{atm}$ in most places, with higher values seen near the coasts, Arctic, and the western Tropical Pacific and Southern Ocean. These standard deviations were considerably smaller than those of the kriging itself (Figs. 6 and A1) but could be significant in a few places especially, but not exclusively, in the Arctic and coastal regions.

5.4 Are some cruises more important than others?

25 It was conceivable that certain cruises dominated the final results. This possibility was studied using the bootstrap method, a statistical technique which permits the assessment of variability in an estimate using just the available data (Wilmott et al., 1985). Bootstrapping creates synthetic sets of data by random resampling from the original data with replacement. We bootstrapped the SOCAT data 10 times by cruise ID to

Deriving a sea surface CO₂ climatology

L. M. Goddijn-Murphy et al.

Title Page

Abstract

Introduction

Conclusions

References

Tables

Figures



Back

Close

Full Screen / Esc

Printer-friendly Version

Interactive Discussion



Deriving a sea surface CO₂ climatology

L. M. Goddijn-Murphy
et al.

Title Page

Abstract

Introduction

Conclusions

References

Tables

Figures

◀

▶

◀

▶

Back

Close

Full Screen / Esc

Printer-friendly Version

Interactive Discussion



estimate the variability of the mean monthly $f_{\text{CO}_2,\text{cl}}$ distributions. The complete SOCAT data set was too big to bootstrap at once. We therefore bootstrapped in two steps, first by cruise ID for each year and region, and then by year and region. Each of the 10 resulting $f_{\text{CO}_2,\text{cl}}$ datasets were kriged as described in Sect. 4 (for each month in each synthetic dataset a different variogram model was fitted and applied). The mean monthly distributions showed that in regions of fewer cruises (outside the North Atlantic and North Pacific) significant variation in $f_{\text{CO}_2,\text{cl}}$ could occur, with up to $50 \mu\text{atm}$ standard deviation (Figs. 8 and A3). It was therefore likely that certain cruises were indeed more important than others. High variability in the east-central equatorial Pacific could be a consequence of not excluding the El Niño years.

5.5 Temporal extrapolation error

The $1.5 \mu\text{atm yr}^{-1}$ rate of change in p_{CO_2} has an estimated precision of $\pm 0.3 \mu\text{atm yr}^{-1}$ (Takahashi et al., 2009) and $\Delta f_{\text{CO}_2,\text{cl}} = \Delta p_{\text{CO}_2,\text{cl}}$ (Eq. 14). The error in $f_{\text{CO}_2,\text{cl}}$ in 2010 due to uncertainty of the $p_{\text{CO}_2,\text{cl}}$ trend was therefore estimated as $\pm (2010 - \text{year}) \cdot 0.3 \mu\text{atm yr}^{-1}$, ranging between $\pm (0.9 - 5.7) \mu\text{atm}$. These extrapolation errors for the month of January and for all months are shown in respective Fig. 9 and Fig. A4. The error was on the high side in the Indian Ocean and in the western Southern Ocean because fewer cruises were performed there in recent times. The absolute monthly mean extrapolation error over all grid points was estimated at $3 \pm 0.1 \mu\text{atm}$ (average over all monthly means \pm standard deviation). This implies that if in reality the rate of change since 1991 was 1.8 instead of $1.5 \mu\text{atm yr}^{-1}$, $f_{\text{CO}_2,\text{cl}}$ would be underestimated by $\sim 3 \mu\text{atm}$ on average. Recent research has shown that this is probable, as Takahashi et al. (2014) present an updated oceanic p_{CO_2} trend of $1.9 \mu\text{atm yr}^{-1}$, a value supported by McKinley et al. (2011).

5.6 Inversion error

Our conversion of $f_{\text{CO}_2,\text{is}}$ to $p_{\text{CO}_2}(T_{\text{eq}})$ could introduce an error if the data was not based on x_{CO_2} analysis (cruise flags not A or B), but on f_{CO_2} calculated from a spectrophotometer, or if the investigator only provided $f_{\text{CO}_2,\text{is}}$ or $p_{\text{CO}_2,\text{is}}$ and did not use Eq. (1) to correct for the temperature difference. This error was assessed by calculating the conversion from $f_{\text{CO}_2,\text{is}}$ to $f_{\text{CO}_2,\text{ym},i}$ using SST and P_{eq} instead of T_{ym} and $P_{\text{eq},\text{ym}}$. This conversion would ideally produce the original SOCAT $f_{\text{CO}_2,\text{is}}$ value. A difference between $f_{\text{CO}_2,\text{is}}$ and “ $f_{\text{CO}_2,\text{ym},i=\text{is}}$ ” implied that our re-computation differed from the one applied by SOCAT or the investigator and we called this difference averaged over one grid box “inversion error”. Note that $\Delta f_{\text{CO}_2,\text{cl}} = \Delta f_{\text{CO}_2,\text{ym}}$. This error turned out in a very small positive bias, negligible in the North Atlantic and other areas with some higher levels in the Southern Ocean (Figs. 10 and A5). The monthly mean inversion bias over all grid points was $1 \pm 0.2 \mu\text{atm}$ (average over all monthly means \pm standard deviation).

5.7 Missing values

A related problem was introduced by missing SOCAT values (Sect. 3.3). Missing values did not always propagate into an inversion error because we made an effort to handle the missing values following SOCAT (Pfeil and Olsen, 2009). If salinity or pressure were missing, SOCAT used EO values for their conversion, reducing systematic $f_{\text{CO}_2,\text{cl}}$ errors in our re-conversion. Missing values of temperature and pressure at the equilibrator could introduce systematic errors, however. It is difficult to estimate the size of these kinds of errors, but Fig. 11 shows the proportion of missing values for January to give an idea about how many data could be affected. The $f_{\text{CO}_2,\text{ym},i}$ calculations were most sensitive to temperature. If T_{eq} was not provided we used in situ SST, so an inversion error would be near zero. However, in these cases $p_{\text{CO}_2,\text{is}}$ was then the starting point of our conversion instead of $p_{\text{CO}_2}(T_{\text{eq}})$ which could lead to significant systematic $f_{\text{CO}_2,\text{ym},i}$ errors. We therefore also reproduced our $f_{\text{CO}_2,\text{cl}}$ distribution maps using only data points with valid T_{eq} values (Figs. 12 and A6). These maps appeared to reveal

Deriving a sea surface CO₂ climatology

L. M. Goddijn-Murphy
et al.

Title Page

Abstract

Introduction

Conclusions

References

Tables

Figures

◀

▶

◀

▶

Back

Close

Full Screen / Esc

Printer-friendly Version

Interactive Discussion



less high $f_{\text{CO}_2,\text{cl}}$ outliers. If only data with valid T_{eq} were selected the data quality was believed to be better, but the number of data points was compromised. The monthly distributions of these data (Fig. A7) therefore showed either lower or higher SD levels. The monthly mean difference $f_{\text{CO}_2,\text{cl}}(\text{all}) - f_{\text{CO}_2,\text{cl}}(\text{valid } T_{\text{eq}})$ ranged between $-3.3 \mu\text{atm}$ (November) and $3.7 \mu\text{atm}$ (January) and was $-0.4 \mu\text{atm}$ on average. The error due to missing values in a monthly distribution file could therefore be interpreted as smaller than about $\pm 3.5 \mu\text{atm}$, resulting in a bias of the annual mean of $-0.4 \mu\text{atm}$.

5.8 Measurement errors

Errors in the SOCAT measurements ($f_{\text{CO}_2,\text{is}}$, T_{eq} , P_{eq} and SST) naturally propagated into $f_{\text{CO}_2,\text{cl}}$ uncertainty. The accuracies for the SOCAT measurements that comply with SOP (Standard Operating Procedures) criteria are given by Pfeil et al. (2013); not all SOCAT data are of this high standard so these accuracies were the highest that could be expected. Likewise the uncertainty in $T_{\text{ym},i}$ had to be taken into account. Ocean-flux GHG gives the SD values and counts with the mean SST_{skin} values from ARC on a $1^\circ \times 1^\circ$ grid; the average standard error ($\text{SD}/\sqrt{\text{count}}$) over all monthly grid boxes that had f_{CO_2} values (all years and months) was ± 0.17 . The uncertainty in the SST difference with subskin SST is ± 0.1 (Donlon et al., 1999). The total uncertainty in $T_{\text{ym},i}$ was therefore estimated to be $\pm 0.2 (\sqrt{0.17^2 + 0.1^2})$. We estimated the propagation of these errors by applying the error for each parameter, x , and calculate $f_{\text{CO}_2,\text{cl}}$. (We calculated $f_{\text{CO}_2,\text{cl}}$ for $x + \Delta x$ and $x - \Delta x$ and $\Delta f_{\text{CO}_2,\text{cl}} = \text{mean} \{ (f_{\text{CO}_2,\text{cl}}(x + \Delta x) - f_{\text{CO}_2,\text{cl}}(x - \Delta x)) / 2 \}$. The results are listed in Table 3. The total error caused by known uncertainties in the parameters was estimated to be $> 3.7 \mu\text{atm} (\sqrt{0.75^2 + 0.015^2 + 2^2 + 3^2})$.

5.9 Summary of errors

The standard deviations of the kriging should account for both spatial variation of the data points and random errors in the $f_{\text{CO}_2,\text{cl}}$ values. The errors caused by the

Deriving a sea surface CO₂ climatology

L. M. Goddijn-Murphy
et al.

Title Page

Abstract

Introduction

Conclusions

References

Tables

Figures

◀

▶

◀

▶

Back

Close

Full Screen / Esc

Printer-friendly Version

Interactive Discussion



7 Conclusions

SOCAT f_{CO_2} (and ρ_{CO_2}) predictions and standard deviations for a reference year 2010, recomputed for a SST suitable for climate change research of air–sea gas exchange and interpolated to a global $1^\circ \times 1^\circ$ grid, have been made available. Two climatology datasets are presented as an online Supplement to this paper, each consisting of 12 monthly NetCDF files: one using all SOCATv1.5 data and one using all data of the recent update SOCATv2. We identified and calculated various possible errors. The errors due to the spatial interpolation, closely related to data density, dominated and some areas showed higher errors of all kinds than others. The data quality/density in the North Atlantic and North Pacific proved to be superior. Our dataset based on SOCAT version 2 is mostly similar to the one based on version 1.5, but if it is used to focus on outliers version 2 should be used because the data quality is better. For future SOCAT versions: it would benefit climatological applications if additional climatological values of f_{CO_2} were directly calculated using the difference between the temperature of sea water in the equilibrator and monthly composite temperatures such as from ARC (Eq. 13), so to avoid the inversion step.

The Supplement related to this article is available online at doi:10.5194/osd-11-1895-2014-supplement.

Acknowledgements. This research is a contribution of the National Centre for Earth Observation, a NERC Collaborative Centre and was supported by the European Space Agency (ESA) Support to Science Element (STSE) project OceanFlux Greenhouse Gases (contract number: 4000104762/11/I-AM). We appreciate the use of the SOCAT data, made available by SOCAT investigators, regional group leaders, quality controllers and data providers.

OSD

11, 1895–1948, 2014

Deriving a sea surface CO₂ climatology

L. M. Goddijn-Murphy et al.

Title Page

Abstract

Introduction

Conclusions

References

Tables

Figures

◀

▶

◀

▶

Back

Close

Full Screen / Esc

Printer-friendly Version

Interactive Discussion



References

- Bakker, D. C. E., Pfeil, B., Smith, K., Hankin, S., Olsen, A., Alin, S. R., Cosca, C., Harasawa, S., Kozyr, A., Nojiri, Y., O'Brien, K. M., Schuster, U., Telszewski, M., Tilbrook, B., Wada, C., Akl, J., Barbero, L., Bates, N. R., Boutin, J., Bozec, Y., Cai, W.-J., Castle, R. D., Chavez, F. P., Chen, L., Chierici, M., Currie, K., de Baar, H. J. W., Evans, W., Feely, R. A., Fransson, A., Gao, Z., Hales, B., Hardman-Mountford, N. J., Hoppema, M., Huang, W.-J., Hunt, C. W., Huss, B., Ichikawa, T., Johannessen, T., Jones, E. M., Jones, S. D., Jutterström, S., Kitidis, V., Körtzinger, A., Landschützer, P., Lauvset, S. K., Lefèvre, N., Manke, A. B., Mathis, J. T., Merlivat, L., Metzl, N., Murata, A., Newberger, T., Omar, A. M., Ono, T., Park, G.-H., Pater-
son, K., Pierrot, D., Ríos, A. F., Sabine, C. L., Saito, S., Salisbury, J., Sarma, V. V. S. S., Schlitzer, R., Sieger, R., Skjelvan, I., Steinhoff, T., Sullivan, K. F., Sun, H., Sutton, A. J., Suzuki, T., Sweeney, C., Takahashi, T., Tjiputra, J., Tsurushima, N., van Heuven, S. M. A. C., Vandemark, D., Vlahos, P., Wallace, D. W. R., Wanninkhof, R., and Watson, A. J.: An update to the Surface Ocean CO₂ Atlas (SOCAT version 2), *Earth Syst. Sci. Data*, 6, 69–90, doi:10.5194/essd-6-69-2014, 2014.
- Dlugokencky, E. J., Masarie, K. A., Lang, P. M., and Tans, P. P.: NOAA Greenhouse Gas Reference from Atmospheric Carbon Dioxide Dry Air Mole Fractions from the NOAA ESRL Carbon Cycle Cooperative Global Air Sampling Network, available at: ftp://aftp.cmdl.noaa.gov/data/trace_gases/co2/flask/surface/ (last access: 27 July 2014), 2014.
- Donlon, C. J., Nightingale, P. D., Sheasby, T., Turner, J., Robinson, I. S., and Emery, J.: Implications of the oceanic thermal skin temperature deviation at high wind speeds, *Geophys. Res. Lett.*, 26, 2505–2508, 1999.
- Donlon, C. J., Minnett, P., Gentemann, C., Nightingale, T. J., Barton, I. J., Ward, B., and Murray, J.: Towards improved validation of satellite sea surface skin temperature measurements for climate research, *J. Climate*, 15, 353–369, 2002.
- Donlon, C., Robinson, I., Casey, K. S., Vazquez-Cuervo, J., Armstrong, E., Arino, O., Gentemann, C., May, D., Leborgne, P., Piollé, J., Barton, I., Beggs, H., Poulter, D. J. S., Merchant, C. J., Bingham, A., Heinz, S., Harris, A., Wick, G., Emery, B., Minnett, P., Evans, R., Llewellyn-Jones, D., Mutlow, C., Reynolds, R. W., Kawamura, H., and Rayner, N.: The GODAE High Resolution Sea Surface Temperature Pilot Project (GHRSSST-PP), *B. Am. Meteorol. Soc.*, 88, 1197–1213, 2007.

Deriving a sea surface CO₂ climatology

L. M. Goddijn-Murphy
et al.

Title Page

Abstract

Introduction

Conclusions

References

Tables

Figures



Back

Close

Full Screen / Esc

Printer-friendly Version

Interactive Discussion



Deriving a sea surface CO₂ climatology

L. M. Goddijn-Murphy
et al.

Title Page

Abstract

Introduction

Conclusions

References

Tables

Figures

◀

▶

◀

▶

Back

Close

Full Screen / Esc

Printer-friendly Version

Interactive Discussion



Emery, W. J., Cherkauer, K., Shannon, B., and Reynolds, R. W.: Hull-mounted sea surface temperatures from ships of opportunity, *J. Atmos. Ocean. Tech.*, 14, 1237–1251, doi:10.1175/1520-0426(1997)014<1237:HMSSTF>2.0.CO;2, 1997.

Emery, W. J., Baldwin, D. J., Schlüssel, P., and Reynolds, R. W.: Accuracy of in situ sea surface temperatures used to calibrate infrared satellite measurements, *J. Geophys. Res.*, 106, 2387–2405, doi:10.1029/2000JC000246, 2001.

Fangohr, S. and Woolf, D. K.: Application of new parameterization of gas transfer velocity and their impact on regional and global marine CO₂ budgets, *J. Marine Syst.*, 66, 195–203, 2007.

Jeffery, C. D., Woolf, D. K., Robinson, I. S., and Donlon, C. J.: One-dimensional modelling of convective CO₂ exchange in the Tropical Atlantic, *Ocean Model.*, 19, 161–182, 2007.

Jeffery, C. D., Robinson, I., Woolf, D. K., and Donlon, C. J.: The response to phase-dependent wind stress and cloud fraction of the diurnal cycle of SST and air–sea CO₂ exchange, *Ocean Model.*, 23, 33–48, 2008.

Kawai, Y. and Wada, A.: Diurnal sea surface temperature variation and its impact on the atmosphere and ocean: a review, *J. Oceanogr.*, 63, 721–744, 2007.

Kennedy, J. J.: A review of uncertainty in in situ measurements and data sets of sea surface temperature, *Rev. Geophys.*, 51, 1–32, doi:10.1002/2013RG000434, 2013.

Kennedy, J. J., Rayner, N. A., Smith, R. O., Saunby, M., and Parker, D. E.: Reassessing biases and other uncertainties in sea-surface temperature observations since 1850 Part 1: Measurement and sampling errors, *J. Geophys. Res.*, 116, D14103, doi:10.1029/2010JD015218, 2011a.

Kennedy, J. J., Rayner, N. A., Smith, R. O., Saunby, M., and Parker, D. E.: Reassessing biases and other uncertainties in sea-surface temperature observations since 1850 Part 2: Biases and homogenisation, *J. Geophys. Res.*, 116, D14104, doi:10.1029/2010JD015220, 2011b.

Kent, E. C., Taylor, P. K., Truscott, B. S., and Hopkins, J. A.: The accuracy of voluntary observing ship's meteorological observations, *J. Atmos. Ocean. Tech.*, 10, 591–608, 1993.

Kettle, H. and Merchant, C. J.: Systematic errors in global air–sea CO₂ flux caused by temporal averaging of sea-level pressure, *Atmos. Chem. Phys.*, 5, 1459–1466, doi:10.5194/acp-5-1459-2005, 2005.

Kettle, H., Merchant, C. J., Jeffery, C. D., Filipiak, M. J., and Gentemann, C. L.: The impact of diurnal variability in sea surface temperature on the central Atlantic air–sea CO₂ flux, *Atmos. Chem. Phys.*, 9, 529–541, doi:10.5194/acp-9-529-2009, 2009.

Deriving a sea surface CO₂ climatology

L. M. Goddijn-Murphy
et al.

Title Page

Abstract

Introduction

Conclusions

References

Tables

Figures



Back

Close

Full Screen / Esc

Printer-friendly Version

Interactive Discussion



- Land, P. E., Shutler, J. D., Cowling, R. D., Woolf, D. K., Walker, P., Findlay, H. S., Upstill-Goddard, R. C., and Donlon, C. J.: Climate change impacts on sea–air fluxes of CO₂ in three Arctic seas: a sensitivity study using Earth observation, *Biogeosciences*, 10, 8109–8128, doi:10.5194/bg-10-8109-2013, 2013.
- 5 Liss, P. S. and Merlivat, L.: Air-sea gas exchange rates: introduction and synthesis, in: *The Role of Air–Sea Exchange in Geochemical Cycling*, edited by: Buat-Menard, P., D Reidel, 113–127, 1986.
- McKinley, G. A., Fay, A. R., Takahashi, T. and Metzl, N.: Convergence of atmospheric and North Atlantic carbon dioxide trends on multidecadal timescales, *Nat Geosci.*, 4, 606–619, doi:10.1038/NGEO1193, 2011.
- 10 Merchant, C. J., Llewellyn-Jones, D., Saunders, R. W., Rayner, N. A., Kent, E. C., Old, C. P., Berry, D., Birks, A. R., Blackmore, T., Corlett, G. K., Embury, O., Jay, V. L., Kennedy, J., Mutlow, C. T., Nightingale, T. J., O’Carroll, A. G., Pritchard, M. J., Remedios, J. J., and Tett, S.: Deriving a sea surface temperature record suitable for climate change research from the along-track scanning radiometers, *Adv. Space Res.*, 41, 1–11, 2008.
- 15 Merchant, C. M., Embury, O., Rayner, N. A., David, I., Berry, D. I., Corlett, G. K., Lean, K., Veal, K. L., Kent, E. C., Llewellyn-Jones, D. T., Remedios, J. J., and Saunders, R.: A 20 year independent record of sea surface temperature for climate from Along-Track Scanning Radiometers, *J. Geophys. Res.*, 117, C12013, doi:10.1029/2012JC008400, 2012.
- 20 O’Carroll, A. G., Eyre, J. R., and Saunders, R. W.: Three-way error analysis between AATSR, AMSR-E, and in situ sea surface temperature observations, *J. Atmos. Ocean. Tech.*, 25, 1197–1207, doi:10.1175/2007JTECHO542.1, 2008.
- Olsen, A., Omar, A. M., Stuart-Menteth, A. C., and Trinanes, J. A.: Diurnal variations of surface ocean *p*CO₂ and sea-air CO₂ flux evaluated using remotely sensed data, *Geophys. Res. Lett.*, 31, L20304, doi:10.1029/2004GL020583, 2004.
- 25 Pebesma, E. J.: *Gstat’s User Manual*, available at: <http://www.gstat.org/gstat.pdf> (last access: 27 February 2013), 1–100, 1999.
- Pfeil, B. and Olsen, A.: A uniform format surface *f*CO₂ database, available at: <http://www.socat.info/publications.html> (last access: 4 June 2012), 1–9, 2009.
- 30 Pfeil, B., Olsen, A., Bakker, D. C. E., Hankin, S., Koyuk, H., Kozyr, A., Malczyk, J., Manke, A., Metzl, N., Sabine, C. L., Akl, J., Alin, S. R., Bates, N., Bellerby, R. G. J., Borges, A., Boutin, J., Brown, P. J., Cai, W.-J., Chavez, F. P., Chen, A., Cosca, C., Fassbender, A. J., Feely, R. A., González-Dávila, M., Goyet, C., Hales, B., Hardman-Mountford, N., Heinze, C., Hood, M.,

Deriving a sea surface CO₂ climatology

L. M. Goddijn-Murphy
et al.

Title Page

Abstract

Introduction

Conclusions

References

Tables

Figures

◀

▶

◀

▶

Back

Close

Full Screen / Esc

Printer-friendly Version

Interactive Discussion



Hoppema, M., Hunt, C. W., Hydes, D., Ishii, M., Johannessen, T., Jones, S. D., Key, R. M., Körtzinger, A., Landschützer, P., Lauvset, S. K., Lefèvre, N., Lenton, A., Lourantou, A., Merlivat, L., Midorikawa, T., Mintrop, L., Miyazaki, C., Murata, A., Nakadate, A., Nakano, Y., Nakaoka, S., Nojiri, Y., Omar, A. M., Padin, X. A., Park, G.-H., Paterson, K., Perez, F. F., Pierrot, D., Poisson, A., Ríos, A. F., Santana-Casiano, J. M., Salisbury, J., Sarma, V. V. S. S., Schlitzer, R., Schneider, B., Schuster, U., Sieger, R., Skjelvan, I., Steinhoff, T., Suzuki, T., Takahashi, T., Tedesco, K., Telszewski, M., Thomas, H., Tilbrook, B., Tjiputra, J., Vandemark, D., Veness, T., Wanninkhof, R., Watson, A. J., Weiss, R., Wong, C. S., and Yoshikawa-Inoue, H.: A uniform, quality controlled Surface Ocean CO₂ Atlas (SOCAT), Earth Syst. Sci. Data, 5, 125–143, doi:10.5194/essd-5-125-2013, 2013.

Reynolds, R. W., Gentemann, C. L., and Corlett, G. K.: Evaluation of AATSR and TMI satellite SST data, J. Climate, 23, 152–165, doi:10.1175/2009JCLI3252.1, 2010.

Sabine, C. L., Hankin, S., Koyuk, H., Bakker, D. C. E., Pfeil, B., Olsen, A., Metzl, N., Kozyr, A., Fassbender, A., Manke, A., Malczyk, J., Akl, J., Alin, S. R., Bellerby, R. G. J., Borges, A., Boutin, J., Brown, P. J., Cai, W.-J., Chavez, F. P., Chen, A., Cosca, C., Feely, R. A., González-Dávila, M., Goyet, C., Hardman-Mountford, N., Heinze, C., Hoppema, M., Hunt, C. W., Hydes, D., Ishii, M., Johannessen, T., Key, R. M., Körtzinger, A., Landschützer, P., Lauvset, S. K., Lefèvre, N., Lenton, A., Lourantou, A., Merlivat, L., Midorikawa, T., Mintrop, L., Miyazaki, C., Murata, A., Nakadate, A., Nakano, Y., Nakaoka, S., Nojiri, Y., Omar, A. M., Padin, X. A., Park, G.-H., Paterson, K., Perez, F. F., Pierrot, D., Poisson, A., Ríos, A. F., Salisbury, J., Santana-Casiano, J. M., Sarma, V. V. S. S., Schlitzer, R., Schneider, B., Schuster, U., Sieger, R., Skjelvan, I., Steinhoff, T., Suzuki, T., Takahashi, T., Tedesco, K., Telszewski, M., Thomas, H., Tilbrook, B., Vandemark, D., Veness, T., Watson, A. J., Weiss, R., Wong, C. S., and Yoshikawa-Inoue, H.: Surface Ocean CO₂ Atlas (SOCAT) gridded data products, Earth Syst. Sci. Data, 5, 145–153, doi:10.5194/essd-5-145-2013, 2013.

Takahashi, T., Sutherland, S. C., Sweeney, C., Poisson, A., Metzl, N., Tilbrook, B., Bates, N., Wanninkhof, R., Feely, R. A., Sabine, C., Olafsson, J., and Nojiri, Y.: Global air–sea CO₂ flux based on climatological surface ocean pCO₂, and seasonal biological and temperature effects, Deep-Sea Res. Pt. II, 45, 1601–1622, 2002.

Takahashi, T., Sutherland, S. C., Wanninkhof, R., Sweeney, C., Feely, R. A., Chipman, D. W., Hales, B., Friederich, G., Chavez, F., Sabine, C., Watson, A., Bakker, D. C. E., Schuster, U., Metzl, N., Yoshikawa-Inoue, H., Ishii, M., Midorikawa, T., Nojiri, Y., Körtzinger, A., Steinhoff, T., Hoppema, M., Olafson, J., Arnarson, T. S., Tilbrook, B., Johannessen, T., Olsen, A.,

Deriving a sea surface CO₂ climatology

L. M. Goddijn-Murphy
et al.

Title Page

Abstract

Introduction

Conclusions

References

Tables

Figures

◀

▶

◀

▶

Back

Close

Full Screen / Esc

Printer-friendly Version

Interactive Discussion



Bellerby, R., Wong, C. S., Delile, B., Bates, N. R., and de Baar, H. J. W.: Climatological mean and decadal change in surface ocean $p\text{CO}_2$, and net sea–air CO_2 flux over the global oceans, *Deep-Sea Res. Pt. II*, 56, 554–577, 2009.

5 Takahashi, T., Sutherland, S. C., Chipman, D. W., Goddard, J. G., and Ho, C.: Climatological distributions of pH, $p\text{CO}_2$, total CO_2 , alkalinity, and CaCO_3 saturation in the global surface Ocean, and temporal changes at selected locations, *Mar. Chem.*, 164, 95–125, doi:10.1016/j.marchem.2014.06.004, 2014.

10 Wanninkhof, R., Asher, W. E., Ho, D. T., Sweeney, C., and McGillis, W. R.: Advances in quantifying air–sea gas exchange and environmental forcing, *Annu. Rev. Mar. Sci.*, 1, 213–44, doi:10.1146/annurev.marine.010908.163742, 2009.

Ward, B., Wanninkhof, R., McGillis, W. R., Jessup, A. T., DeGrandpre, M. D., Hare, J. E., and Edson, J. B.: Biases in the air–sea flux of CO_2 resulting from ocean surface temperature gradients, *J. Geophys. Res.*, 109, C08S08, doi:10.1029/2003JC001800, 2004.

15 Weiss, R. F.: Carbon dioxide in water and seawater: the solubility of a non-ideal gas, *Mar. Chem.*, 2, 203–215, 1974.

Wilmott, C. J., Ackleson, S. G., Davis, R. E., Feddema, J. J., Klink, K. M., Legates, D. R., O'Donnell, J., and Rowe, C.: Statistics for the evaluation and comparison of models, *J. Geophys. Res.*, 90, 8995–9005, 1985.

Deriving a sea surface CO₂ climatology

L. M. Goddijn-Murphy
et al.

Title Page

Abstract

Introduction

Conclusions

References

Tables

Figures

◀

▶

◀

▶

Back

Close

Full Screen / Esc

Printer-friendly Version

Interactive Discussion



Table 1. Differences between Takahashi climatology and climatology presented in this paper.

	Takahashi et al. (2009)	This study
Reference year	2000	2010
Resolution	4° × 5°	1° × 1°
Data	Excludes El Niño and coastal data	Includes El Niño and coastal data
Spatial Interpolation	Involves continuity equation based on a 2-D diffusion–advection transport equation for surface waters	Simple block kriging without continuity equation
Parameter	p_{CO_2} (= f_{CO_2})	f_{CO_2} (and p_{CO_2})
f_{CO_2} taken at	instantaneous intake temperature SST _{depth}	monthly composite sub skin SST from ARC

Deriving a sea surface CO₂ climatology

L. M. Goddijn-Murphy
et al.

Title Page

Abstract

Introduction

Conclusions

References

Tables

Figures



Back

Close

Full Screen / Esc

Printer-friendly Version

Interactive Discussion



Table 2. The different kriging options that were applied to the monthly data sets of $f_{\text{CO}_2, \text{cl}}$ for 2010; ordinary block kriging was applied with min, max, radius, dx and dy as explained in Sect. 4.

min	max	radius	dx	dy
4	20	60	5	5
4	20	40	5	5
4	20	100	5	5
4	20	60	1	1
4	20	60	10	10
4	10	60	5	5
4	40	60	5	5
2	20	60	5	5
10	20	60	5	5

Deriving a sea surface CO₂ climatology

L. M. Goddijn-Murphy
et al.

Title Page

Abstract

Introduction

Conclusions

References

Tables

Figures



Back

Close

Full Screen / Esc

Printer-friendly Version

Interactive Discussion



Table 3. Error estimations of the parameters involved in the $f_{\text{CO}_2,\text{cl}}$ computation and their consequent errors $\Delta f_{\text{CO}_2,\text{cl}}$ (μatm).

Parameter x	error	$\Delta f_{\text{CO}_2,\text{cl}}$
ΔSST	$\pm 0.05^*$	± 0.75
ΔT_{eq}	$\pm 0.05^*$	± 0.015
ΔP_{eq}	$\pm 0.5^*$	~ 0
$\Delta f_{\text{CO}_2,\text{is}}$	$\pm 2^*$	± 2
$\Delta T_{\text{ym},i}$	± 0.2	± 3

* for SOP data (Pfeil et al., 2013).

Deriving a sea surface CO₂ climatology

L. M. Goddijn-Murphy
et al.

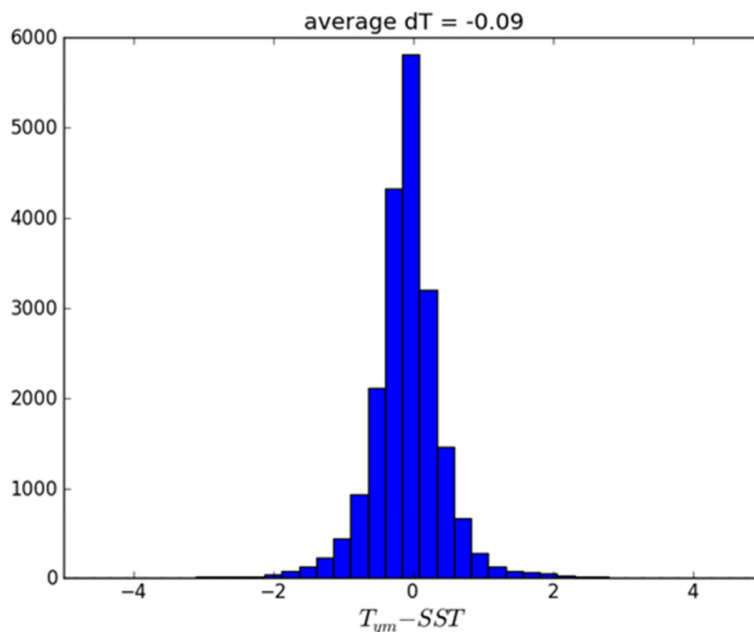
[Title Page](#)[Abstract](#)[Introduction](#)[Conclusions](#)[References](#)[Tables](#)[Figures](#)[Back](#)[Close](#)[Full Screen / Esc](#)[Printer-friendly Version](#)[Interactive Discussion](#)

Figure 1. Histogram of temperature difference between monthly gridded data of subskin SST derived from ARC, T_{ym} , and in situ SST from SOCAT version 1.5 using global data from all available years.

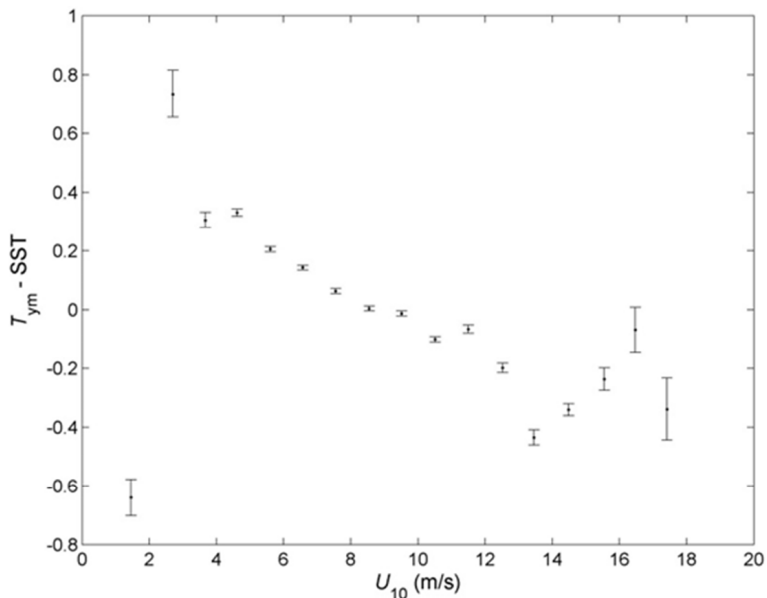


Figure 2. Scatter plot of temperature difference between monthly gridded data of subskin SST derived from ARC, T_{ym} , and in situ SST from SOCAT version 1.5, using data from all available years in the North Atlantic, binned in 1 m s^{-1} U_{10} bins. The error bar indicates the standard error of the mean.

Deriving a sea surface CO₂ climatology

L. M. Goddijn-Murphy et al.

Title Page	
Abstract	Introduction
Conclusions	References
Tables	Figures
◀	▶
◀	▶
Back	Close
Full Screen / Esc	
Printer-friendly Version	
Interactive Discussion	



Deriving a sea surface CO₂ climatology

L. M. Goddijn-Murphy
et al.

Title Page

Abstract

Introduction

Conclusions

References

Tables

Figures



Back

Close

Full Screen / Esc

Printer-friendly Version

Interactive Discussion

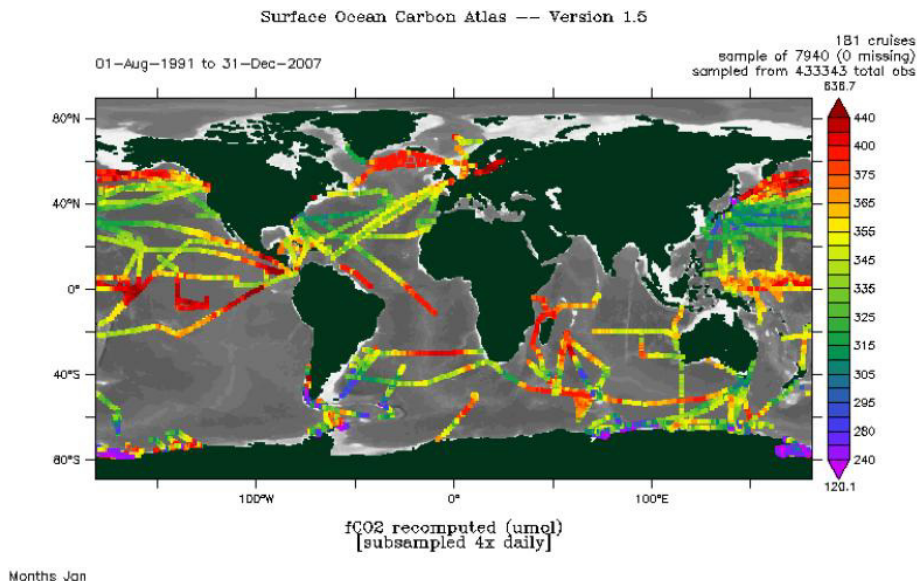


Figure 3. SOCAT CO₂ fugacity (µatm) data shown in the online Cruise Data Viewer for the month January; all data from 1 August 1991 to 31 December 2007.

Deriving a sea surface CO₂ climatology

L. M. Goddijn-Murphy et al.

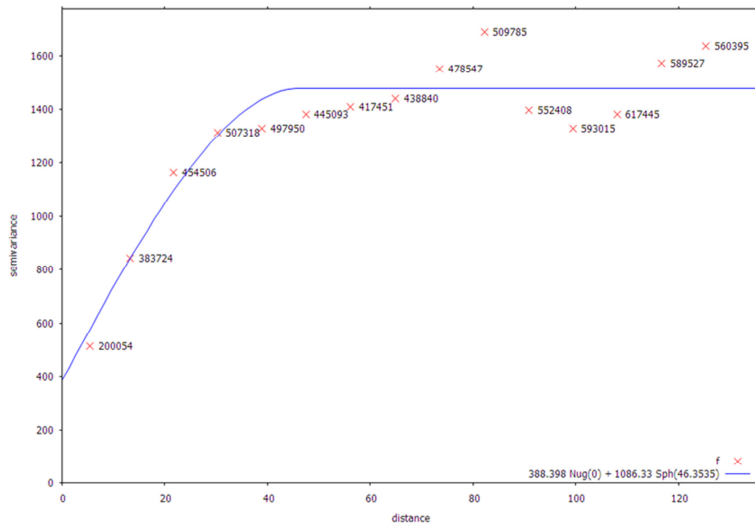


Figure 4. Variogram for global $f_{CO_2,cl}$ data in 2010 for the month January, derived from $f_{CO_2,is}$ shown in Fig. 3. The numbers next to each data point are the number of data pairs.

Title Page

Abstract Introduction

Conclusions References

Tables Figures

◀ ▶

◀ ▶

Back Close

Full Screen / Esc

Printer-friendly Version

Interactive Discussion



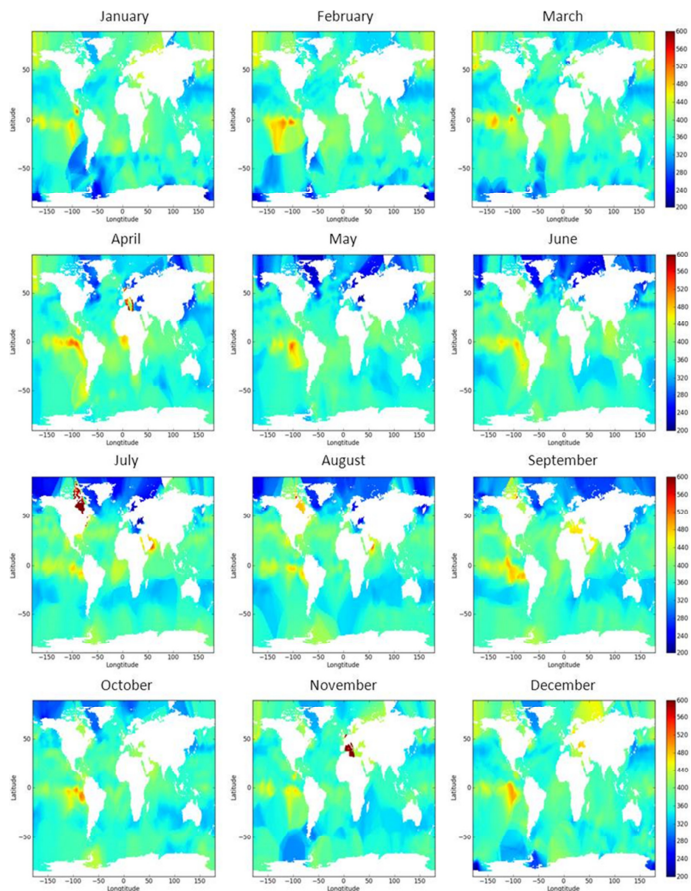


Figure 5. Monthly $f_{\text{CO}_2,\text{cl}}$ values in the global oceans estimated for 2010 for January (top left) to December (bottom right) on a 200–600 μatm scale; data were interpolated to a $1^\circ \times 1^\circ$ grid using ordinary block kriging with $\text{min} = 4$, $\text{max} = 20$, $\text{radius} = 60$ and $\text{block size} = 5 \times 5$.

Deriving a sea surface CO_2 climatology

L. M. Goddijn-Murphy et al.

Title Page

Abstract Introduction

Conclusions References

Tables Figures

◀ ▶

◀ ▶

Back Close

Full Screen / Esc

Printer-friendly Version

Interactive Discussion



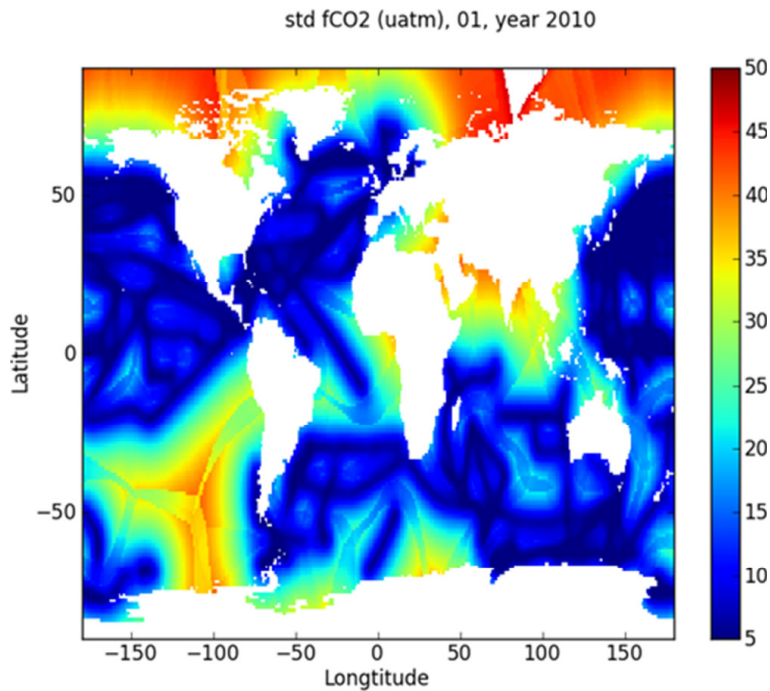


Figure 6. Standard deviation in $f_{\text{CO}_2,\text{cl}}$ estimated for January 2010 on a 5 to 50 μatm scale, associated with the ordinary block kriging shown in Fig. 5.

Deriving a sea surface CO₂ climatology

L. M. Goddijn-Murphy et al.

Title Page

Abstract

Introduction

Conclusions

References

Tables

Figures



Back

Close

Full Screen / Esc

Printer-friendly Version

Interactive Discussion



Deriving a sea surface CO₂ climatology

L. M. Goddijn-Murphy
et al.

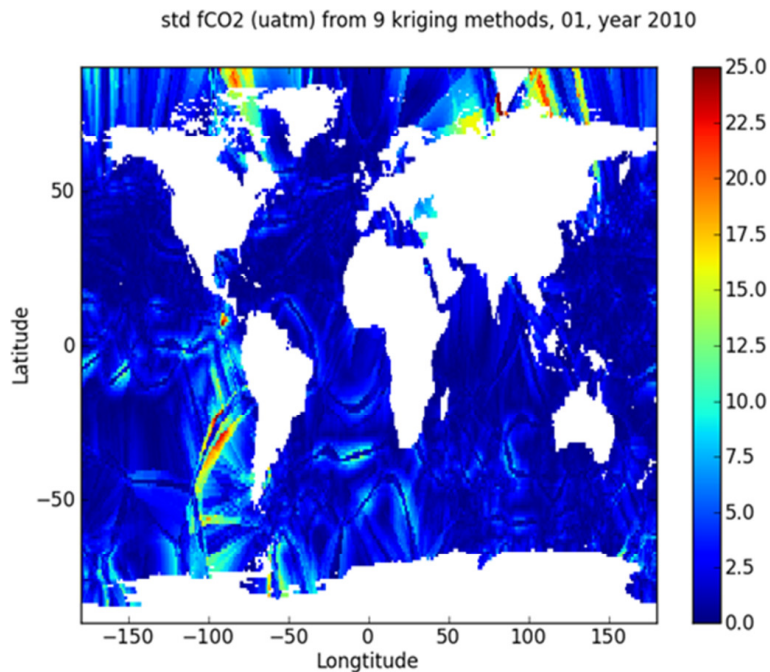
[Title Page](#)[Abstract](#)[Introduction](#)[Conclusions](#)[References](#)[Tables](#)[Figures](#)[Back](#)[Close](#)[Full Screen / Esc](#)[Printer-friendly Version](#)[Interactive Discussion](#)

Figure 7. Standard deviations of the mean over nine different kriging results of $f_{\text{CO}_2,\text{cl}}$ estimated for January 2010, using the range of options shown in Table 2; on a 0 to 25 μatm scale.

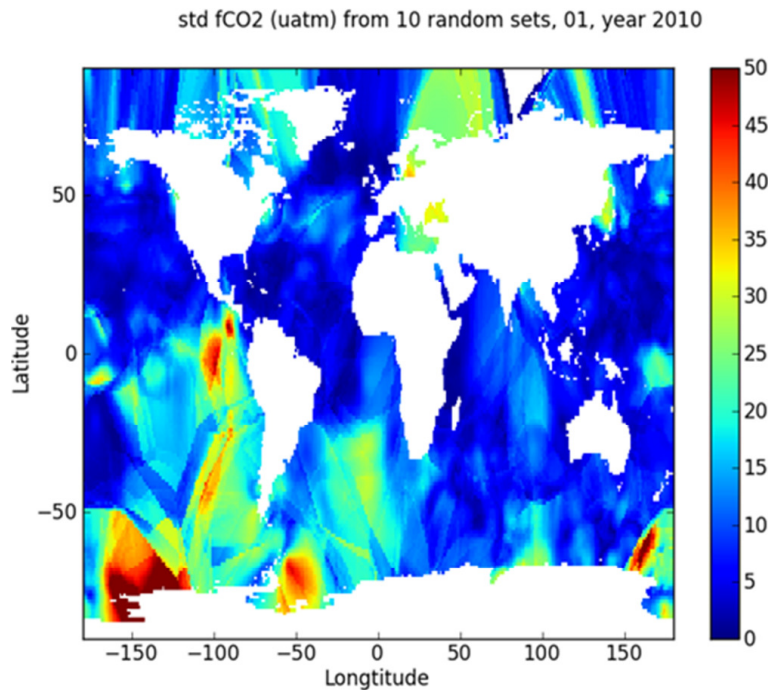


Figure 8. Standard deviations of the mean over 10 bootstrapped datasets of $f_{\text{CO}_2, \text{cl}}$ estimated for January 2010; on a 0 to 50 μatm scale.

Deriving a sea surface CO₂ climatology

L. M. Goddijn-Murphy et al.

Title Page

Abstract	Introduction
Conclusions	References
Tables	Figures

◀	▶
◀	▶

Back	Close
------	-------

Full Screen / Esc

Printer-friendly Version

Interactive Discussion



Deriving a sea surface CO₂ climatology

L. M. Goddijn-Murphy
et al.

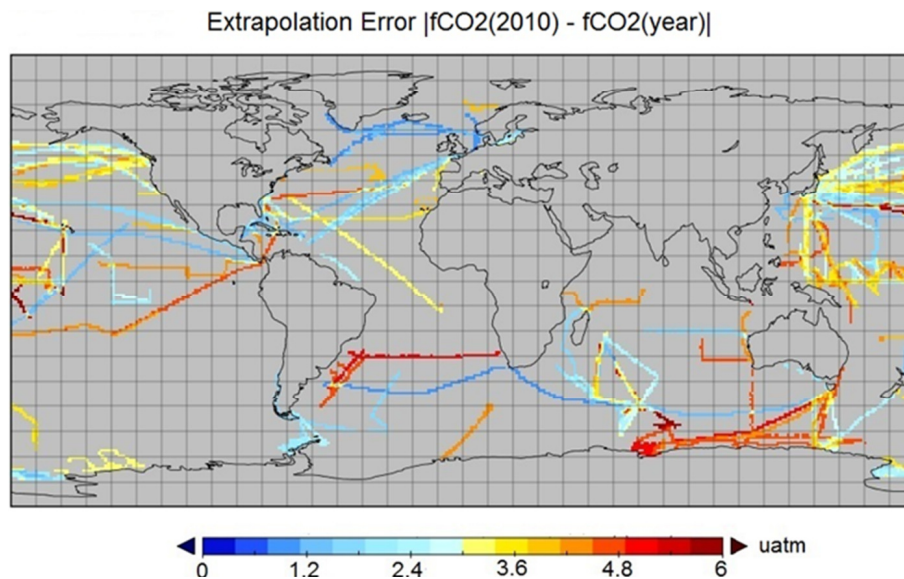


Figure 9. Calculated propagation of the “temporal extrapolation error” in $f_{\text{CO}_2,\text{cl}}$ estimated for January 2010 due to uncertainty in p_{CO_2} trend; on a 0 to 6 μatm scale.

[Title Page](#)[Abstract](#)[Introduction](#)[Conclusions](#)[References](#)[Tables](#)[Figures](#)[◀](#)[▶](#)[◀](#)[▶](#)[Back](#)[Close](#)[Full Screen / Esc](#)[Printer-friendly Version](#)[Interactive Discussion](#)

Deriving a sea surface CO₂ climatology

L. M. Goddijn-Murphy
et al.

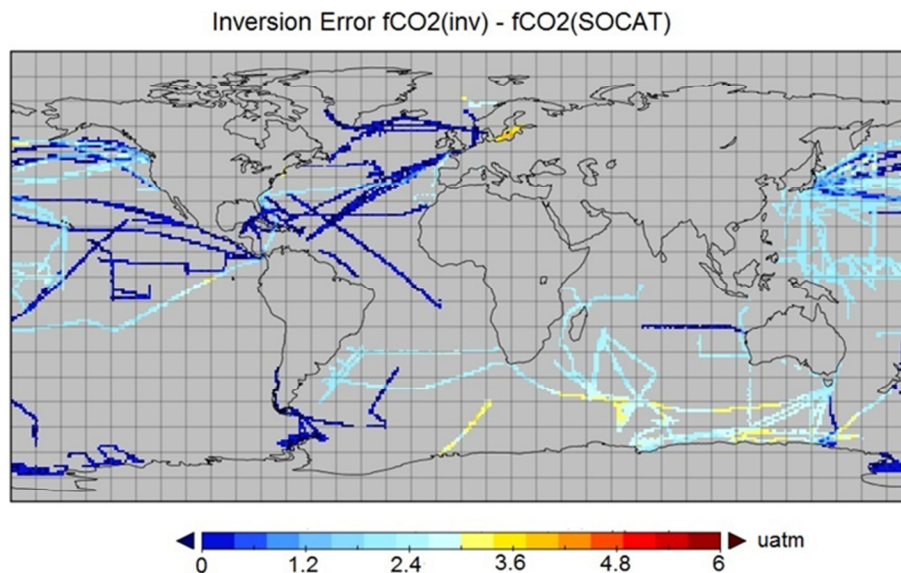


Figure 10. Calculated “inversion error” in $f_{\text{CO}_2,\text{cl}}$ estimated for January 2010, on a 0 to 6 μatm scale.

[Title Page](#)[Abstract](#)[Introduction](#)[Conclusions](#)[References](#)[Tables](#)[Figures](#)[Back](#)[Close](#)[Full Screen / Esc](#)[Printer-friendly Version](#)[Interactive Discussion](#)

Deriving a sea surface CO₂ climatology

L. M. Goddijn-Murphy
et al.

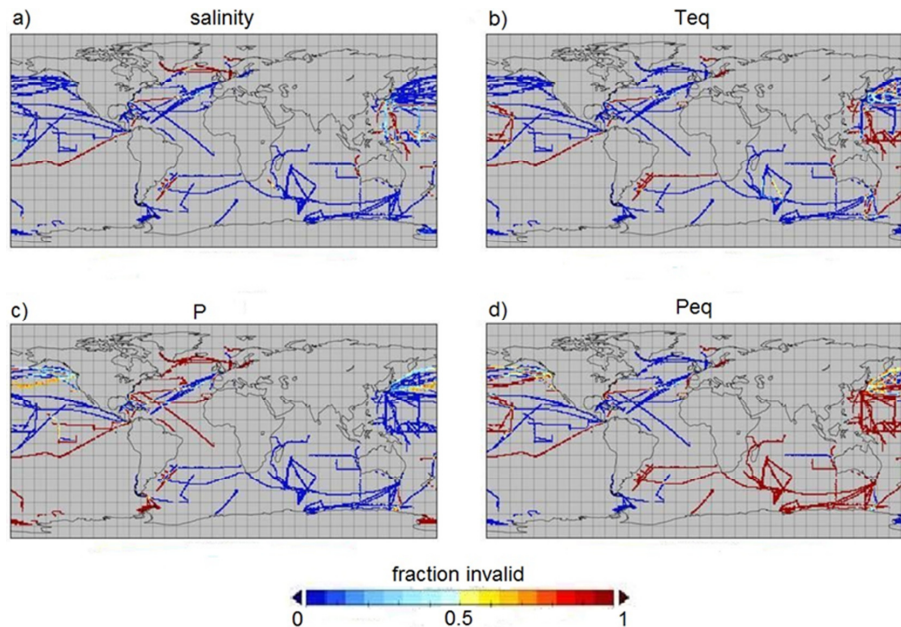


Figure 11. Fractions of $f_{\text{CO}_2, \text{cl}}$ estimated for January 2010, calculated with missing value (a) salinity, (b) T_{eq} , (c) P , and (d) P_{eq} ; on a 0 to 1 scale.

[Title Page](#)[Abstract](#)[Introduction](#)[Conclusions](#)[References](#)[Tables](#)[Figures](#)[◀](#)[▶](#)[◀](#)[▶](#)[Back](#)[Close](#)[Full Screen / Esc](#)[Printer-friendly Version](#)[Interactive Discussion](#)

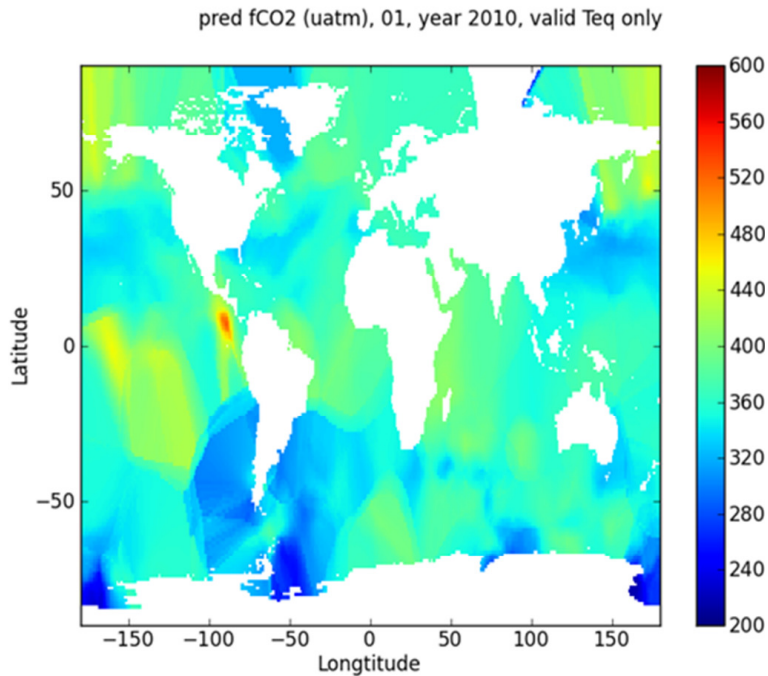


Figure 12. As Fig. 5, January, but using only data points with valid T_{eq} .

Deriving a sea surface CO₂ climatology

L. M. Goddijn-Murphy et al.

Title Page	
Abstract	Introduction
Conclusions	References
Tables	Figures
◀	▶
◀	▶
Back	Close
Full Screen / Esc	
Printer-friendly Version	
Interactive Discussion	



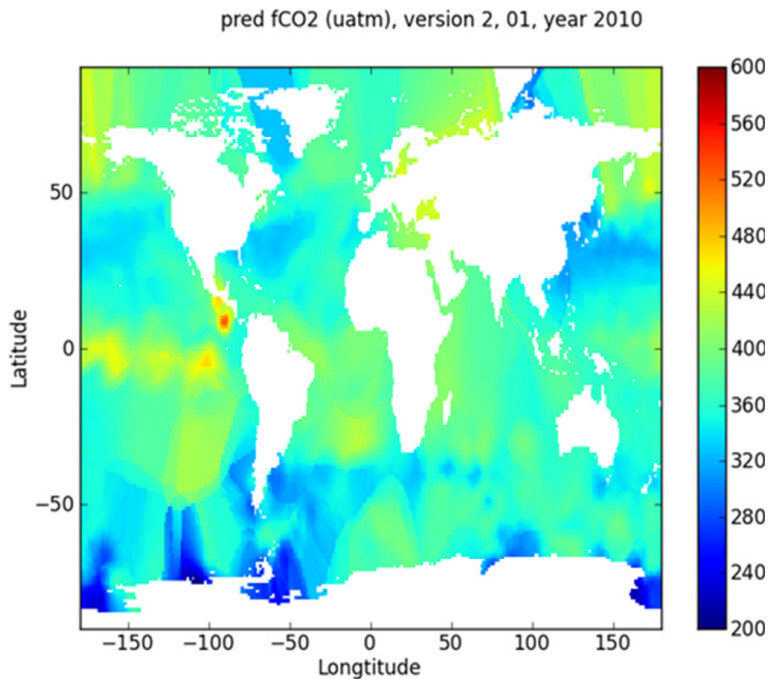


Figure 13. As Fig. 5, January, but using SOCAT version 2 data.

OSD

11, 1895–1948, 2014

Deriving a sea surface CO₂ climatology

L. M. Goddijn-Murphy et al.

Title Page

Abstract

Introduction

Conclusions

References

Tables

Figures

◀

▶

◀

▶

Back

Close

Full Screen / Esc

Printer-friendly Version

Interactive Discussion



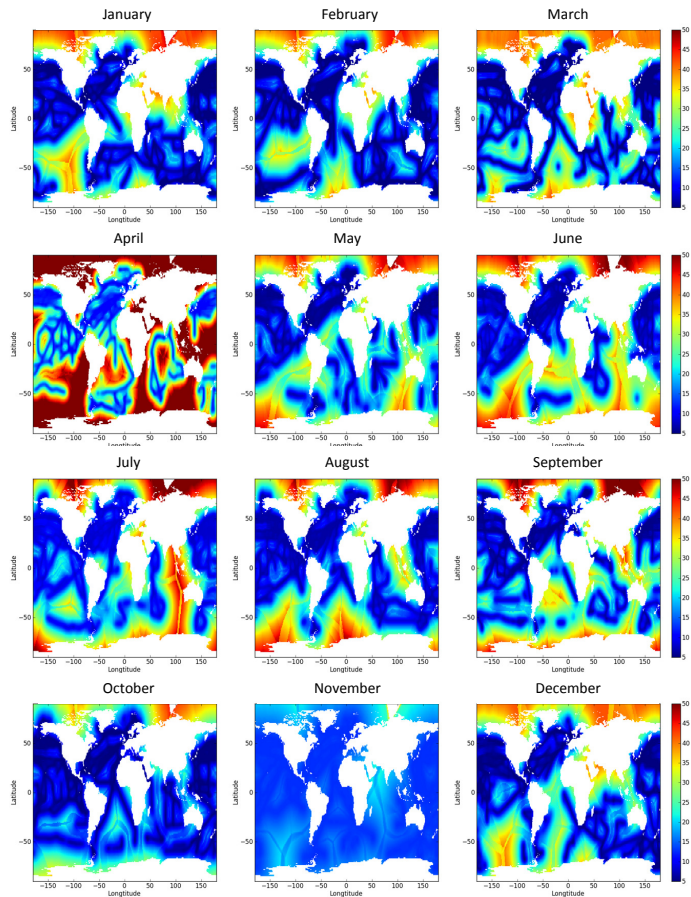


Figure A1. Spatial interpolation errors in estimations of $f_{\text{CO}_2, \text{cl}}$ in 2010. Standard deviation in $f_{\text{CO}_2, \text{cl}}$ estimated for 2010 associated with the ordinary block kriging results shown in Fig. 5; on a 5 to 50 μatm scale.

Deriving a sea surface CO₂ climatology

L. M. Goddijn-Murphy et al.

Title Page

Abstract Introduction

Conclusions References

Tables Figures

◀ ▶

◀ ▶

Back Close

Full Screen / Esc

Printer-friendly Version

Interactive Discussion



Deriving a sea surface CO₂ climatology

L. M. Goddijn-Murphy
et al.

Title Page

Abstract

Introduction

Conclusions

References

Tables

Figures



Back

Close

Full Screen / Esc

Printer-friendly Version

Interactive Discussion

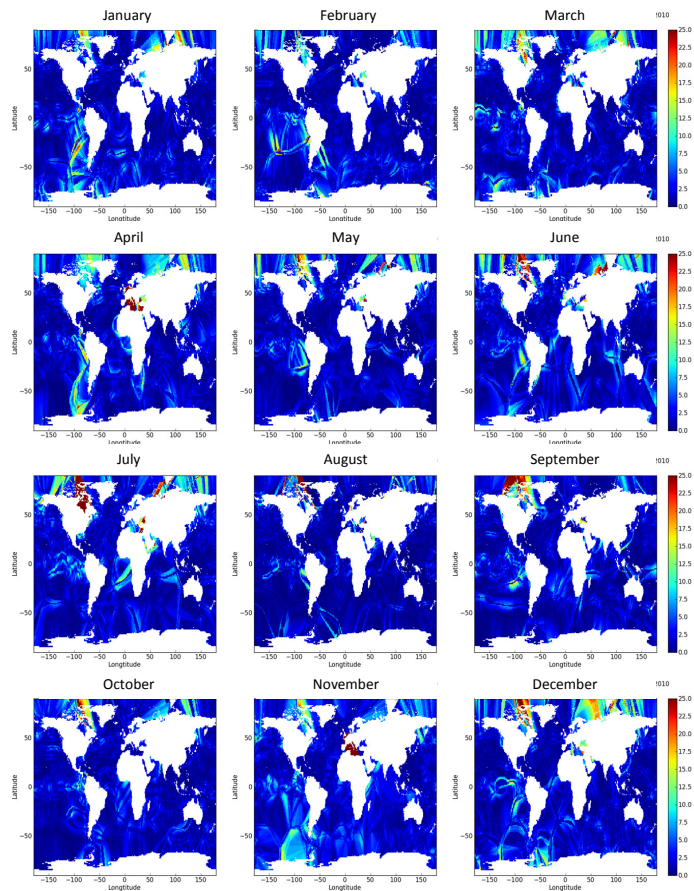


Figure A2. Variation in $f_{\text{CO}_2,\text{cl}}$ in 2010 distributions due to different kriging approaches. Standard deviations of the mean over the different kriging results of $f_{\text{CO}_2,\text{cl}}$ estimated for 2010, using the range of options shown in Table 1; on a 0 to 25 μatm scale.

Deriving a sea surface CO₂ climatology

L. M. Goddijn-Murphy
et al.

Title Page

Abstract

Introduction

Conclusions

References

Tables

Figures



Back

Close

Full Screen / Esc

Printer-friendly Version

Interactive Discussion

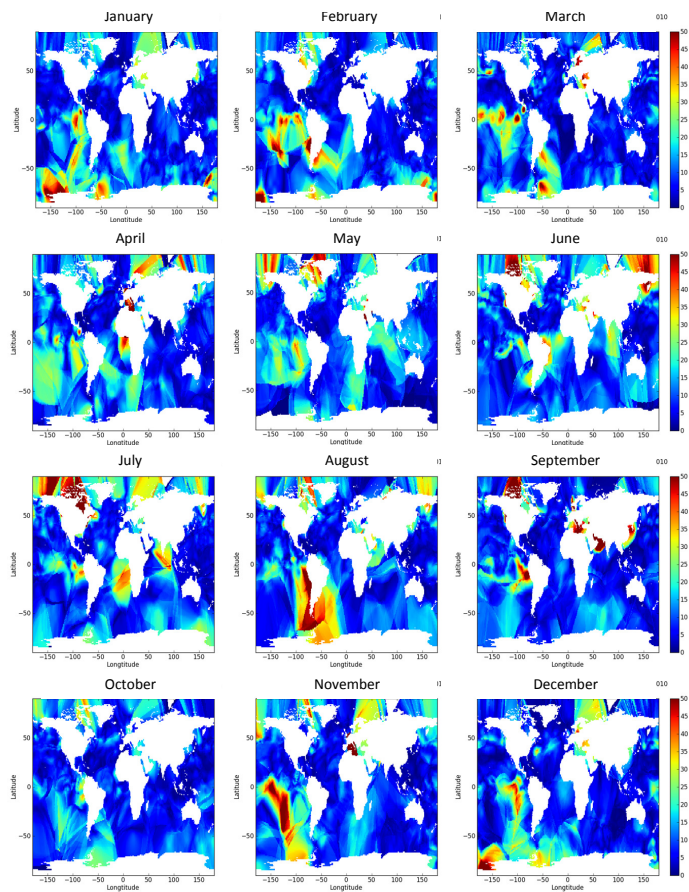


Figure A3. Errors in $f_{\text{CO}_2,\text{cl}}$ in 2010 by bootstrapping cruises. Standard deviations of the mean over 10 bootstrapped datasets of $f_{\text{CO}_2,\text{cl}}$ estimated 2010; on a 0 to 50 μatm scale.

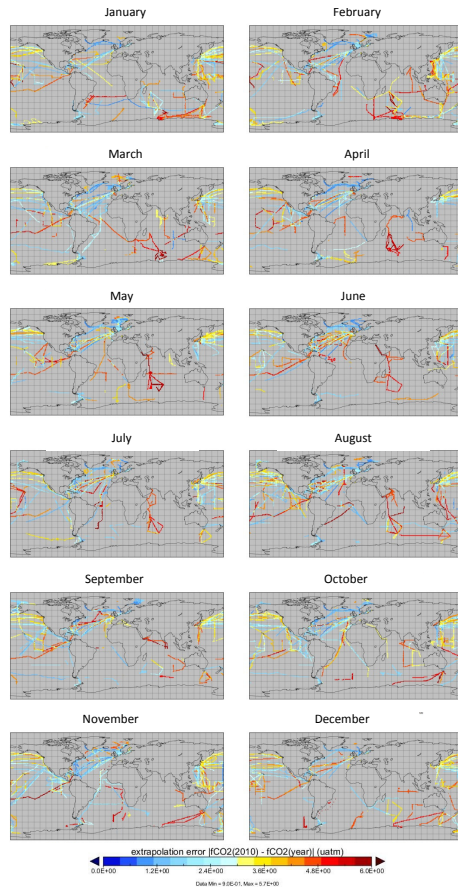


Figure A4. Estimated errors in $f_{\text{CO}_2,\text{cl}}$ in 2010 due to the extrapolation to the year 2010. Calculated propagation of the “temporal extrapolation error” in $f_{\text{CO}_2,\text{cl}}$ estimated for 2010 due to uncertainty in p_{CO_2} trend, on a 0 to 6 μatm scale.

Deriving a sea surface CO₂ climatology

L. M. Goddijn-Murphy et al.

Title Page

Abstract Introduction

Conclusions References

Tables Figures

◀ ▶

◀ ▶

Back Close

Full Screen / Esc

Printer-friendly Version

Interactive Discussion



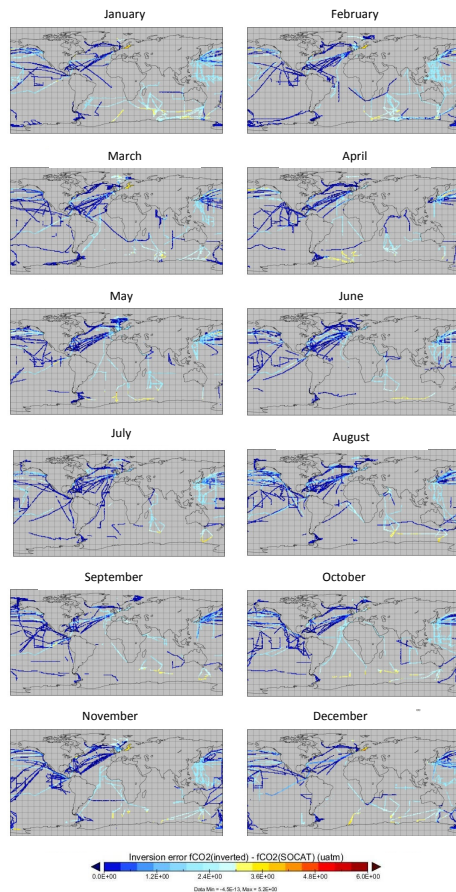


Figure A5. Estimated errors in $f_{\text{CO}_2,\text{cl}}$ in 2010 due to the inversion step. Calculated propagation of the “inversion error” in $f_{\text{CO}_2,\text{cl}}$ estimated for 2010, on a 0 to 6 μatm scale.

Deriving a sea surface CO₂ climatology

L. M. Goddijn-Murphy et al.

Title Page

Abstract Introduction

Conclusions References

Tables Figures

◀ ▶

◀ ▶

Back Close

Full Screen / Esc

Printer-friendly Version

Interactive Discussion



Deriving a sea surface CO₂ climatology

L. M. Goddijn-Murphy
et al.

Title Page

Abstract

Introduction

Conclusions

References

Tables

Figures



Back

Close

Full Screen / Esc

Printer-friendly Version

Interactive Discussion

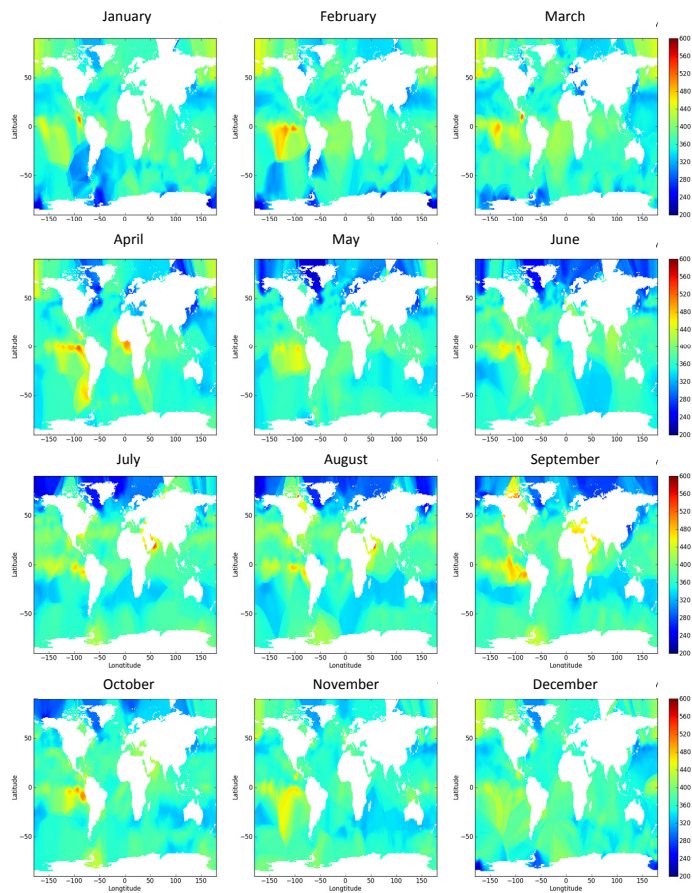


Figure A6. Monthly global distributions of $f_{\text{CO}_2,\text{cl}}$ in 2010, using data points with T_{eq} only. As Fig. 5, but for data points with valid T_{eq} values only.

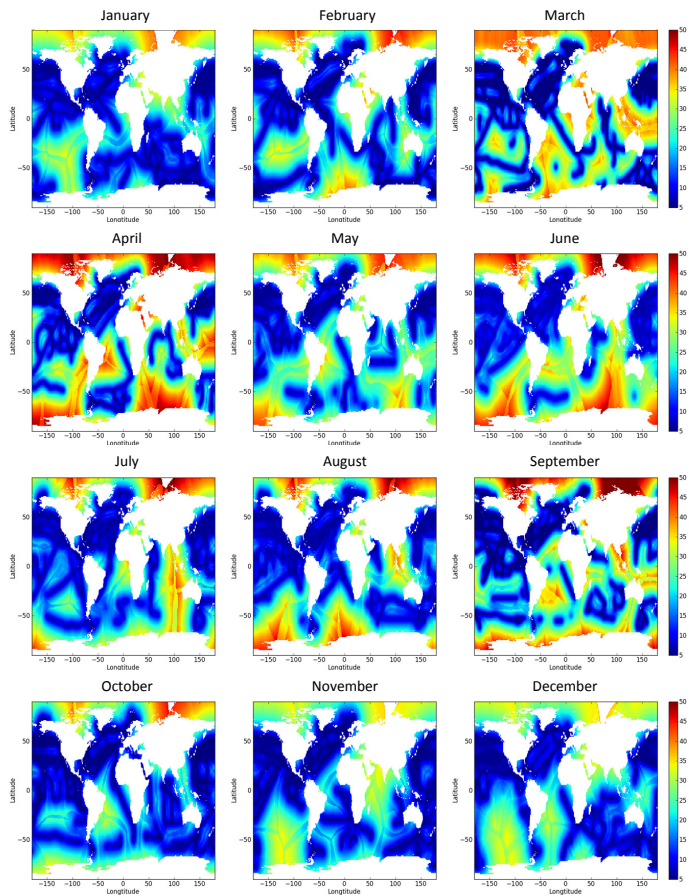


Figure A7. Spatial interpolation errors in estimations of $f_{\text{CO}_2, \text{cl}}$ in 2010, using data points with T_{eq} only. As Fig. A1, but for data points with valid T_{eq} values only.

Deriving a sea surface CO₂ climatology

L. M. Goddijn-Murphy et al.

Title Page

Abstract Introduction

Conclusions References

Tables Figures

⏪ ⏩

◀ ▶

Back Close

Full Screen / Esc

Printer-friendly Version

Interactive Discussion



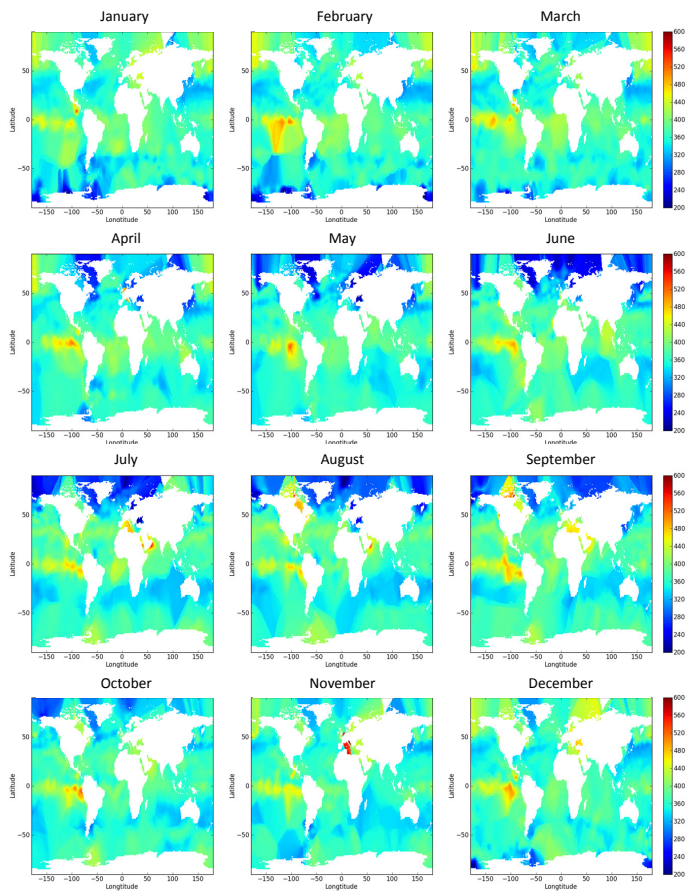


Figure A8. Monthly global distributions of $f_{\text{CO}_2,\text{cl}}$ in 2010 from SOCAT version 2. As Fig. 5, but for SOCAT version 2 instead of version 1.5.

Deriving a sea surface CO₂ climatology

L. M. Goddijn-Murphy et al.

Title Page	
Abstract	Introduction
Conclusions	References
Tables	Figures
◀	▶
◀	▶
Back	Close
Full Screen / Esc	
Printer-friendly Version	
Interactive Discussion	



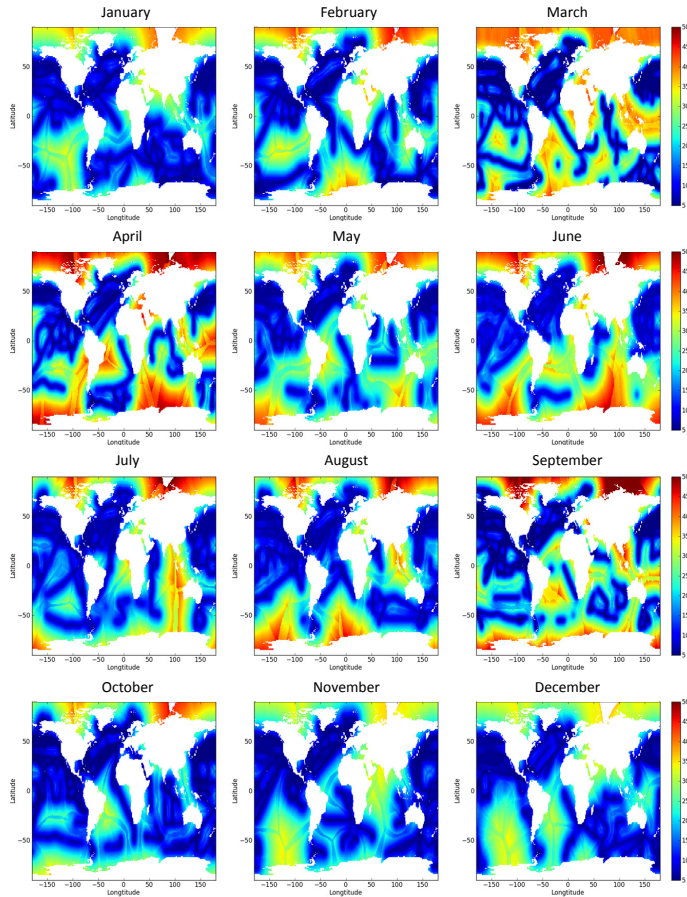


Figure A9. Spatial interpolation errors in $f_{\text{CO}_2,\text{cl}}$ in 2010 using SOCAT version 2. As Fig. A1, but for SOCAT version 2 instead of version 1.5.

Deriving a sea surface CO₂ climatology

L. M. Goddijn-Murphy et al.

Title Page

Abstract Introduction

Conclusions References

Tables Figures

◀ ▶

◀ ▶

Back Close

Full Screen / Esc

Printer-friendly Version

Interactive Discussion

